NUREG/CR-3305
LA-9776-MS

Comparison of BEACON and COMPARE Reactor Cavity Subcompartment Analyses

Prepared by M. W. Burkett, E. S. Idar, R. G. Gido,
J. F. Lime, A. Koestel

Los Alamos National Laboratory

Prepared for
U.S. Nuclear Regulatory
Commission

8405220096 840430
PDR NUREG
CR-3305 R PDR

NOTICE

This report was prepared as an account of work sponsored by an agency of the United States Government. Neither the United States Government nor any agency thereof, or any of their employees, makes any warranty, expressed or implied, or assumes any legal liability of responsibility for any third party's use, or the results of such use, of any information, apparatus, product or process disclosed in this report, or represents that its use by such third party would not infringe privately owned rights.

NOTICE

Availability of Reference Materials Cited in NRC Publications

Most documents cited in NRC publications will be available from one of the following sources:

1. The NRC Public Document Room, 1717 H Street, N.W.
   Washington, DC 20555
2. The NRC/GPO Sales Program, U.S. Nuclear Regulatory Commission,
   Washington, DC 20555
3. The National Technical Information Service, Springfield, VA 22161

Although the listing that follows represents the majority of documents cited in NRC publications, it is not intended to be exhaustive.

Referenced documents available for inspection and copying for a fee from the NRC Public Document Room include NRC correspondence and internal NRC memoranda; NRC Office of Inspection and Enforcement bulletins, circulars, information notices, inspection and investigation notices; Licensee Event Reports; vendor reports and correspondence; Commission papers; and applicant and licensee documents and correspondence.

The following documents in the NUREG series are available for purchase from the NRC/GPO Sales Program: formal NRC staff and contractor reports, NRC-sponsored conference proceedings, and NRC booklets and brochures. Also available are Regulatory Guides, NRC regulations in the *Code of Federal Regulations*, and *Nuclear Regulatory Commission Issuances*.

Documents available from the National Technical Information Service include NUREG series reports and technical reports prepared by other federal agencies and reports prepared by the Atomic Energy Commission, forerunner agency to the Nuclear Regulatory Commission.

Documents available from public and special technical libraries include all open literature items, such as books, journal and periodical articles, and transactions. *Federal Register* notices, federal and state legislation, and congressional reports can usually be obtained from these libraries.

Documents such as theses, dissertations, foreign reports and translations, and non-NRC conference proceedings are available for purchase from the organization sponsoring the publication cited.

Single copies of NRC draft reports are available free, to the extent of supply, upon written request to the Division of Technical Information and Document Control, U.S. Nuclear Regulatory Commission, Washington, DC 20555.

Copies of industry codes and standards used in a substantive manner in the NRC regulatory process are maintained at the NRC Library, 7920 Norfolk Avenue, Bethesda, Maryland, and are available there for reference use by the public. Codes and standards are usually copyrighted and may be purchased from the originating organization or, if they are American National Standards, from the American National Standards Institute, 1430 Broadway, New York, NY 10018.

GPO Printed copy price: $4.00

NUREG/CR-3305
LA-9776-MS

Comparison of BEACON and COMPARE Reactor Cavity Subcompartment Analyses

Manuscript Completed: February 1984
Date Published: April 1984

Prepared by
M. W. Burkett E. S. Idar, R. G. Gido,
J. F. Lime, A. Koestel*

Los Alamos National Laboratory
Los Alamos, NM 87545

*Consultant at Los Alamos
Box 108 Patagonia Star Route
Nogales, AZ 85621

Prepared for
Division of Systems Integration
Office of Nuclear Reactor Regulation
U. S. Nuclear Regulatory Commission
Washington, D.C. 20555
NRC FIN A7265

An Affirmative Action/Equal Opportunity Employer

Edited by Mary Timmers, Group Q-6

NOTICE

This report was prepared as an account of work sponsored by an agency of the United States Government. Neither the United States Government nor any agency thereof, or any of their employees, makes any warranty, expressed or implied, or assumes any legal liability or responsibility for any third party's use, or the results of such use, of any information, apparatus, product or process disclosed in this report, or represents that its use by such third party would not infringe privately owned rights.

COMPARISON OF BEACON AND COMPARE REACTOR CAVITY SUBCOMPARTMENT ANALYSES

by

M. W. Burkett, E. S. Idar, R. G. Gido, J. F. Lime, and A. Koestel

ABSTRACT

In this study, a more advanced "best-estimate" containment code, BEACON-MOD3A, was used to calculate force and moment loads resulting from a high-energy blowdown for two reactor cavity geometries previously analyzed with the licensing computer code COMPARE-MOD1A. The BEACON force and moment loads were compared with the COMPARE results to determine the safety margins provided by the COMPARE code. The forces and moments calculated by the codes were found to be different, although not in any consistent manner, for the two reactor cavity geometries studied. Therefore, generic summary statements regarding margins cannot be made because of the effects of the detailed physical configuration. However, differences in the BEACON and COMPARE calculated forces and moments can be attributed to differences in the modeling assumptions used in the codes and the analyses.

I. INTRODUCTION

Utilities submitting applications to the United States Nuclear Regulatory Commission (NRC) to construct and operate nuclear power plants are required to prove that the plants' containment structures are designed to withstand the pressure and temperature conditions resulting from loss-of-coolant (LOCA), steam-line break, or feedwater-line break accidents. Computer codes often are used to determine the pressure and temperature distributions within the containment subcompartments that result from the high-energy blowdown of water and/or steam of these postulated accidents. The analyses involve determining the differential pressure build-up between subcompartments for blowdowns within the containment and also determining the forces and moments acting on the reactor vessel from blowdowns within the reactor cavity. The NRC review of the applicant's analyses includes confirmatory analyses with a licensing code such as COMPARE-MOD1A.[1,2] To solve the multidimensional, transient, two-phase fluid flow problem, COMPARE uses several simplifying assumptions that generally result in calculated pressure values that are higher (that is, more conservative) than those that actually would occur. Primarily, the flow field is assumed to be one-dimensional, homogenous, and in equilibrium. (The COMPARE

assumptions are evaluated analytically in Ref. 3.) Several advanced best-estimate containment analysis codes such as BEACON-MOD3A[4] are capable of calculating a multidimensional, two-phase, nonhomogenous, nonequilibrium flow field. Therefore, it is important to evaluate the differences in calculated results between the licensing code (COMPARE) and the more recently developed advanced code (BEACON) to assess the margin of conservatism provided by the licensing calculations.

Previous analytical studies with the BEACON and COMPARE codes have established application procedures for both codes relevant to subcompartment analyses.[5,6] In addition, comparisons between calculated results and experimental data for the Battelle-Frankfurt containment tests[6,7] have shown that COMPARE calculations are conservative (that is, COMPARE calculates higher differential pressure values) relative to BEACON calculations and test data and that the BEACON calculations are an improved representation of the complex flow field developed as a result of a blowdown within the containment.

The objective of this study was to assess the margin of conservatism in previously calculated reactor vessel forces and moments by the COMPARE code for blowdowns within representative reactor cavity geometries.[5] Because no supporting experimental data for this type of problem were available, the assessment was performed by comparing the COMPARE-calculated forces and moments with the forces and moments calculated by the BEACON code for the same reactor cavity geometries. The objective also includes evaluating the differences in the two codes' calculations relative to the simplifying assumptions made in the COMPARE code.

Section II of this report discusses the reactor cavity subcompartment analyses performed with the BEACON code. (BEACON-calculated forces and moments are shown and compared with COMPARE calculations.) The differences between the two codes' calculations relative to equilibrium assumptions in the COMPARE code are evaluated in Sec. III. In addition, the possible effects of turbulent jet diffusion on subcompartment analyses are discussed. Appendix A shows the BEACON models and input decks for the reactor cavity subcompartment analysis discussed in Sec. II, and Appendix B presents BEACON and COMPARE models and input decks

A. Description of the COMPARE/MOD1A Computer Code

The COMPARE/MOD1A computer code was developed specifically to perform subcompartment transient response analyses of nuclear power plants, including those with ice condensers, and the NRC recognizes it as a licensing tool to perform such analyses. The subcompartments are represented as volumes that are connected by junctions. The volume thermodynamics and flow equations are for a homogeneous mixture assumed to be in thermodynamic equilibrium and consisting of any one or any combination of (a) steam, (b) water, and (c) any three perfect gases. Flow between volumes can be based on (a) compressible (polytropic or isentropic) orifice flow of an ideal gas-like mixture that can be used to approximate the homogeneous equilibrium flow model, (b) Moody flow with an arbitrary multiplier, and (c) a one-dimensional solution of the momentum equation that includes an accounting for the effects of inertia. Variable-area doors and heat sinks also can be modeled, but they were not used . these analyses. The COMPARE code capabilities have been extended so that overall containment and hydrogen-burning analyses can be performed.[8]

B. Description of the BEACON/MOD3A Computer Code

BEACON is a best-estimate, advanced containment code developed by EG G Idaho, Inc., at the Idaho National Engineering Laboratory (INEL) for the NRC.The current version of the code is BEACON/MOD3A, which incorporates all of

the developments to date and is suitable for analyzing the short-term behavior of multicompartment containment systems, including heat transfer to surrounding walls. However, all BEACON (and COMPARE) calculations in this report ignore heat transfer to surrounding walls.

BEACON represents an advance over other containment system analysis codes like COMPARE because it incorporates more realistic modeling features. In addition to providing lumped-parameter homogeneous flow modeling as in COMPARE and other existing containment codes, BEACON provides one- and two-dimensional Eulerian (that is, the computing mesh is fixed in the flow domain), nonhomogeneous, and nonequilibrium flow-modeling capabilities. When using the BEACON "best-estimate" (BEST) option, mechanical and thermal near-equilibrium between phases are assumed by setting (internally in the code) the interphasic drag and heat-transfer coefficients to very large values. These assumptions have produced good code/data comparisons for certain Battelle-Frankfurt containment experiments. However, a considerable amount of chemical nonequilibrium exists between the phases (flashing) for most practical problems, and it is treated correctly in the code. A greater degree of mechanical and thermal nonequilibrium can be modeled by using the USERDEF option instead of the BEST option. In this case, the analyst should be cautious when using very low values of interphasic drag or heat-transfer coefficients when the void fraction is approaching zero or unity because the code tends to be unstable under these conditions. All these additional capabilities allow more sophisticated formulations of many important containment analysis problems that cannot be analyzed with the other codes.

Table I is a brief comparison of the characteristics of the COMPARE and BEACON codes. Previously developed containment codes have used the lumped-parameter approach in which only a single set of average properties is used to describe the flow field in a large volume. BEACON maintains this and adds the capability to examine the details of a two-component, two-phase flow field in one or two dimensions under nonhomogeneous, nonequilibrium conditions (unequal velocities and/or unequal temperatures between the two phases). This added capability allows the analysis of problems such as the calculation of the jet

TABLE I

COMPARISON OF COMPARE AND BEACON CONTAINMENT ANALYSIS CODES

Feature	COMPARE/MOD1A	BEACON/MOD3A
Containment applications	Subcompartment analysis	Subcompartment analysis
Compartment model	Lumped-parameter	Lumped-parameter and Eulerian mesh
Flow model	Two-phase, homogeneous between phases, one-dimensional	Two-phase, unequal velocity between phases, two-dimensional
Thermodynamic model	Complete equilibrium between phases	Nonequilibrium between phases

impact forces of a fluid leaving a pipe break, the variation in flow properties as air is displaced from a compartment by steam and water, the water entrainment or de-entrainment by a high-speed vapor flow, the flow of a flashing liquid, and many other complex nonequilibrium problems found in containment system analysis. See Ref. 4 for additional details.

C. Description of the Force-Moment Calculations

At the present time, BEACON-MOD3A does not have the capability to calculate forces and moments for reactor cavity subcompartment geometries. Instead of modifying the existing BEACON code, we decided to use the force-moment capability available in COMPARE-MOD1A. That is, the BEACON-calculated reactor cavity pressure distribution was used as the input condition to the COMPARE force-moment calculation algorithm.

As discussed in Ref. 5, COMPARE converts the pressure acting on the reactor vessel surface to a force vector. The projected area of the curved surface (force-moment surface area) multiplied by the pressure acting on that surface gives the magnitude of the net force vector acting normal to the projected surface area through its area centroid. Moments are determined from the forces and the corresponding moment arm vectors associated with the forces. The moment arm vector is defined as the perpendicular vector distance from the moment axis to the force vector line of action. A detailed description of the COMPARE force-moment calculative procedure is available in Refs. 2 and 5.

The pressure contributions of the BEACON cells composing a single COMPARE force-moment surface were determined by weighting the individual cell pressures with the cell volume. The volume-weighted cell pressures were used to obtain an average BEACON presssure for the COMPARE force-moment surface. These average BEACON pressures were used to determine the reactor cavity forces and moments.

II. REACTOR CAVITY SUBCOMPARTMENT ANALYSIS

A. Reactor Cavity Models

BEACON models were developed for both reactor cavities according to the geometry established in the COMPARE base-case models (Ref. 5). That is, the BEACON models generally used the COMPARE flow areas and fluid volumes. However, a basic difference between the two codes (multidimensional vs one-dimensional) often made this difficult to achieve, but flow areas and fluid volumes agree quite well in most cases. By basing the BEACON models on the COMPARE base-case geometry, a more accurate evaluation of the margin of conservatism provided by the COMPARE code could be made for the geometries under investigation.

Two reactor cavity geometries, designated as Geometry 1 and Geometry 2 in Ref. 5, were investigated using BEACON. The postulated LOCA for Geometry 1 was a double-ended hot-leg break within the annulus (the region between the shield wall and the pressure vessel). The annulus region for this geometry is sealed at the top and has a restricted exit to the lower reactor cavity [Figs. 1(a) and 1(b)]. The distance between the shield wall and pressure vessel is approximately 0.9 m (3.0 ft). Neutron detectors are located within the annulus.

In Geometry 2, a 0.093-m^2 (1.0-ft^2) cold-leg break was assumed to occur within the shield-wall penetration [Figs. 2(a) and 2(b)]. The annulus region for this geometry is open at the top and has no restricted opening to the lower reactor cavity. The gap between the shield wall and the pressure vessel is 0.2 m (0.5 ft). There are no neutron detectors located within the annulus.

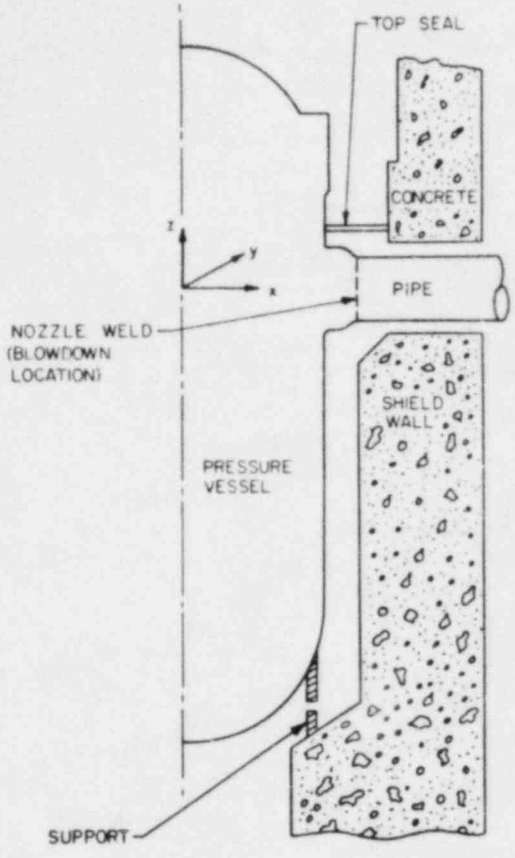

Fig. 1(a).
Geometry 1 reactor cavity vertical (x-z) cross section.

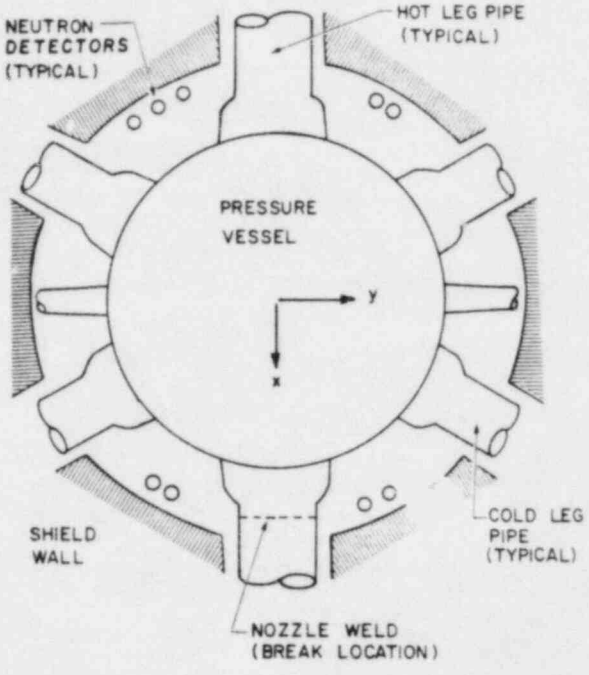

Fig. 1(b).
Geometry 1 reactor cavity horizontal (x-y) cross section.

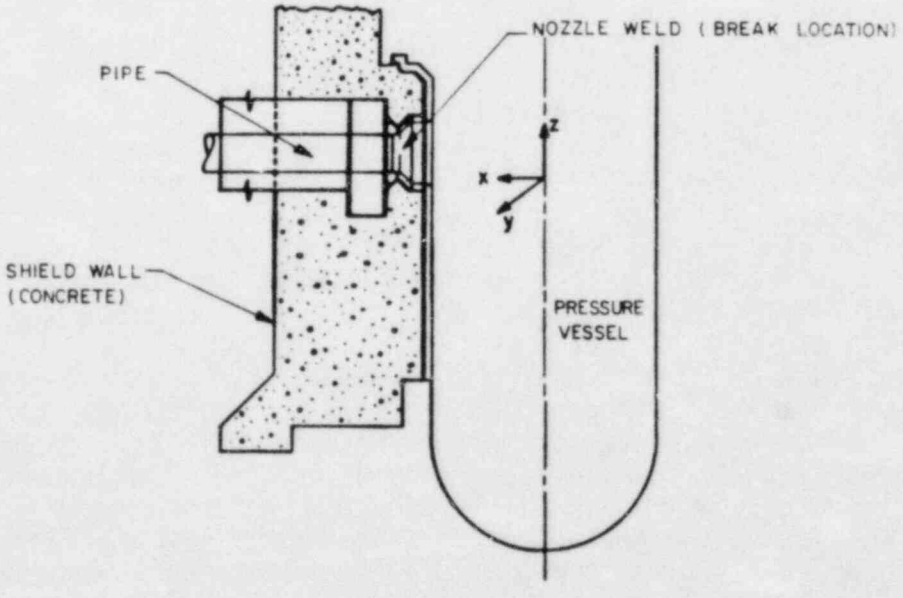

Fig. 2(a).
Geometry 2 reactor cavity vertical cross section showing break location within the shield wall.

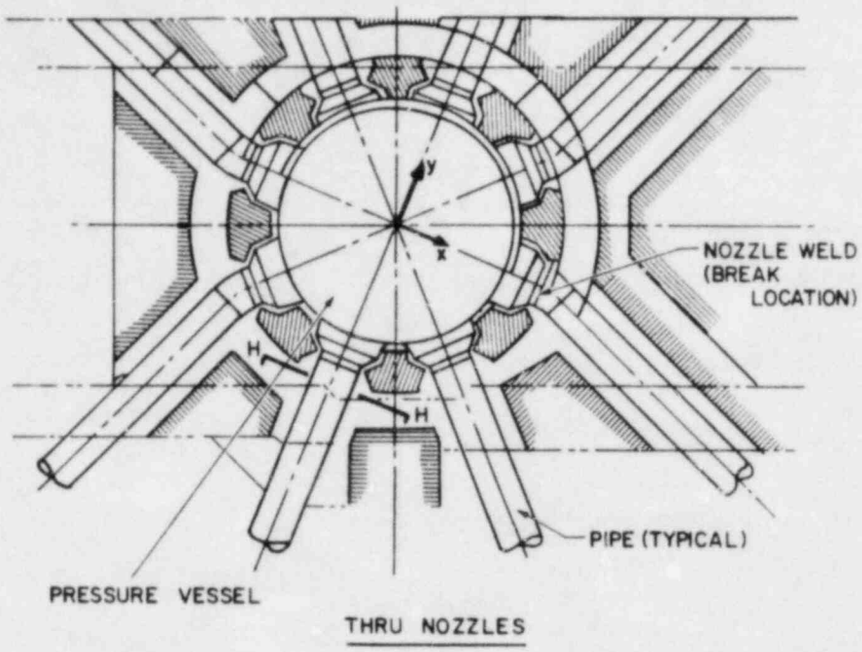

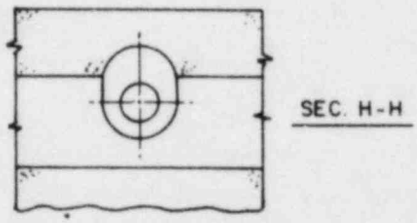

Fig. 2(b).
Geometry 2 reactor cavity horizontal cross section through the nozzles.

1. Description of the BEACON Model for Geometry 1. The BEACON model for Geometry 1 was established using the COMPARE base-case noding diagrams. Because the break occurred within the annulus, only one model, which used most of the available modeling options in BEACON, was necessary. The annulus was modeled as an unwrapped 19- by 9-cell Cartesian mesh of uniform depth. COMPARE flow areas and fluid volumes were achieved by using the partial flow blockage and obstacle cell options in BEACON. The walls of the unwrapped cavity mesh were modeled as rigid/slip boundaries.

The annular flow regions that exist along the hot- and cold-leg pipe penetrations were modeled with the out-of-plane flow option. One-dimensional out-of-plane cells (meshes) connected the upper portion of the unwrapped cavity mesh to a large lumped-parameter region representing the upper and lower containment. The restricted exit or skirt opening to the lower reactor cavity was modeled with four one-dimensional cells (meshes). These cells were positioned along the bottom of the unwrapped cavity and provided access to the lower reactor cavity containment. The blowdown or break was modeled as a liquid source located within the unwrapped annulus mesh. The model geometry and the BEACON input deck are found in Appendix A.

2. Description of the BEACON Model for Geometry 2. In Geometry 2, the break was located within the shield-wall penetration. The source location required two BEACON models--one for the shield-wall blowdown region and one for the unwrapped cavity (annulus). The shield-wall model would determine the blowdown mass flow and enthalpy vs time that would enter the annulus region. The shield-wall penetration to reactor cavity annulus mass flow rates determined by the shield-wall model calculation were used as the source data for the unwrapped cavity model. BEACON Eulerian region coupling methods and blowdown location restrictions prevented modeling this reactor cavity geometry as one interconnected system.

The shield-wall penetration model was composed of a single 17- by 26-cell axisymmetric mesh with radial offset. Obstacle cells were used to achieve the COMPARE base-case flow areas and volumes while preserving the geometry of the shield-wall/cold-leg region. The walls of the mesh and the obstacle cell surfaces were modeled as rigid/slip boundaries. Also, a constant-pressure exterior boundary condition was specified along the lower mesh opening, and an outflow boundary was specified along a portion of the top wall.

The BEACON reactor cavity annulus model for Geometry 2 also was established using the COMPARE base-case noding information provided. The unwrapped annulus was modeled as a 23- by 17-cell Cartesian mesh of uniform depth. As in Geometry 1, COMPARE flow areas and fluid volumes were obtained by using the partial flow blockage and obstacle cell options in BEACON. The left and right walls of the annulus mesh were modeled as rigid/slip boundaries, and a major portion of the top boundary was modeled as a constant pressure boundary to represent the connection between the annulus and the upper containment. The entire lower boundary of the unwrapped annulus mesh was joined to a 23- by 1-cell Cartesian mesh representing the lower reactor cavity. Two additional meshes (modeling skirt openings) provided for the opening from the lower reactor cavity to the lower containment. The upper and lower containments were modeled as two lumped-parameter regions. Three one-dimensional, out-of-plane meshes modeling the annular flow passage along the primary system pipes connected the upper portion of the unwrapped annulus mesh to the upper containment. The blowdown was located in the unwrapped annulus mesh. The BEACON models and input decks for the shield-wall penetration and reactor cavity for Geometry 2 also are in Appendix A.

The ability to model a break location in detail is an added advantage of the BEACON code. Instead of being restricted to using only form-loss coefficients to model abrupt area changes or unusual geometries, a close approximation of the actual geometry can be obtained with BEACON. For this particular geometry, we were able to obtain the COMPARE model flow area and fluid volumes without compromising the actual geometry of the shield-wall penetration region. A comparison of the computer-generated BEACON model and the actual shield-wall penetration geometry is presented in Figs. 3(a) and 3(b).

B. Comparison of BEACON- and COMPARE-Calculated Forces and Moments

1. Geometry 1 Force-Moment Comparison. The comparisons between the BEACON and COMPARE base-case geometry forces and moments are presented in Figs. 4(a) and 4(b), respectively. COMPARE calculated a maximum x-direction force of -34.2 MN at 0.025 s and a maximum moment about the y-axis of 60.1 MN-m at 0.025 s. BEACON calculated a maximum x-force of -24.0 MN between 0.01 s and 0.015 s and a maximum y-moment of -82.5 MN-m between 0.0375 and 0.045 s. The significant difference between the COMPARE and BEACON force-moment profiles can be attributed to the differences in the calculated pressure field distributions

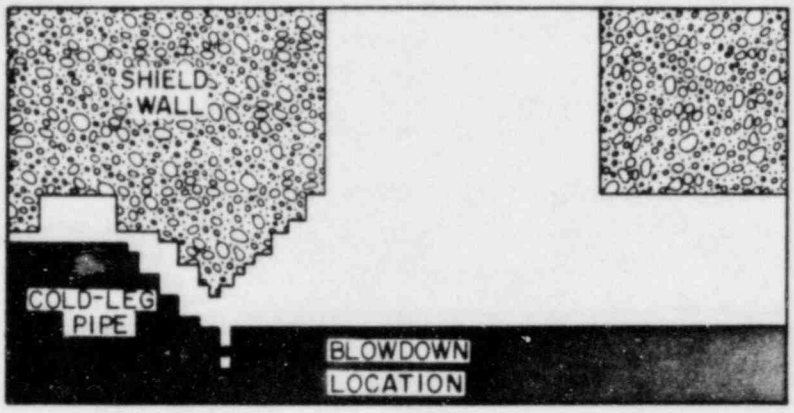

Fig. 3(a).
Computer-generated BEACON model of the shield-wall penetration region for Geometry 2.

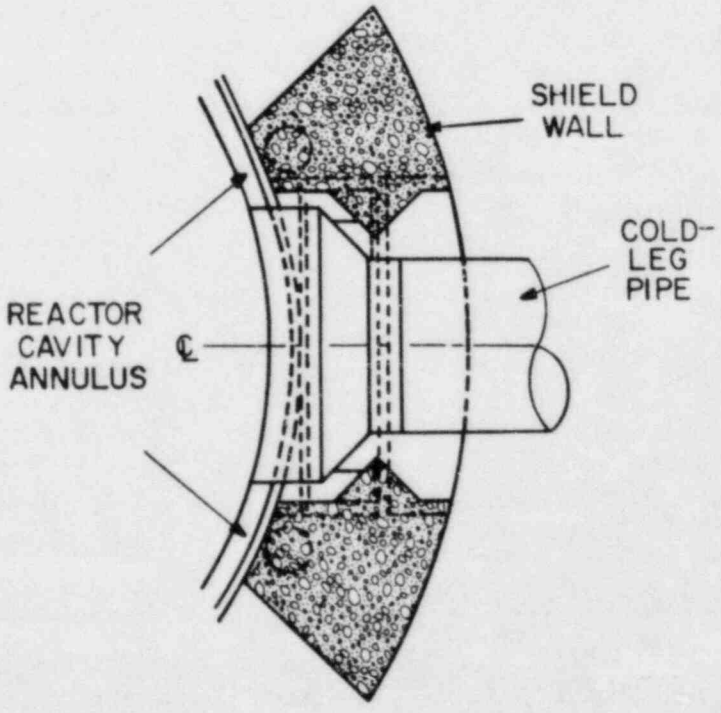

Fig. 3(b).
Shield-wall penetration plan view of annulus at the reactor nozzle.

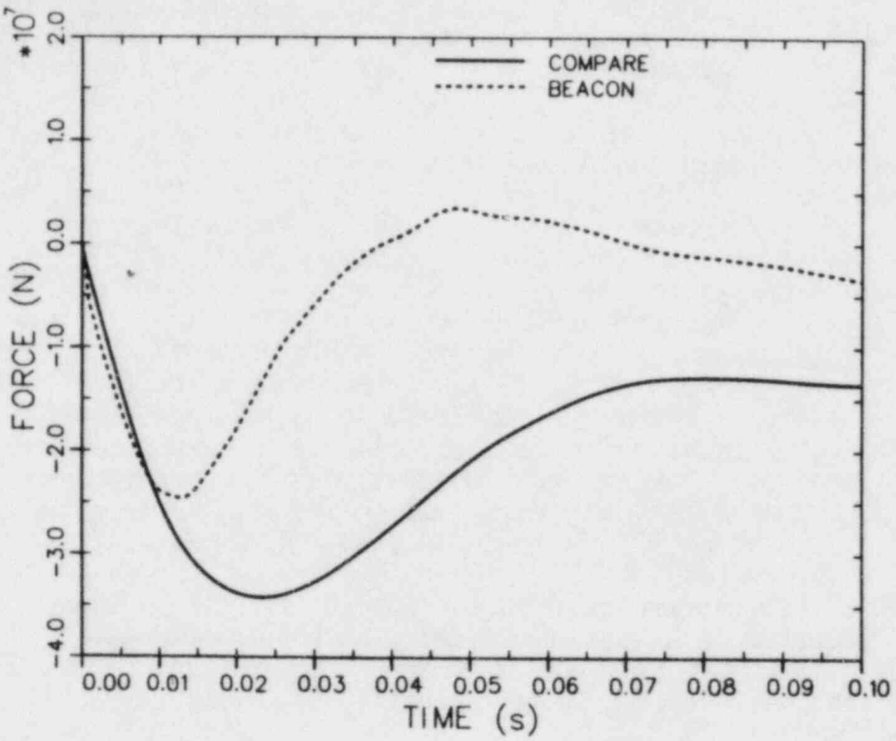

Fig. 4(a).
Comparison of COMPARE- and BEACON-calculated x-forces for Geometry 1.

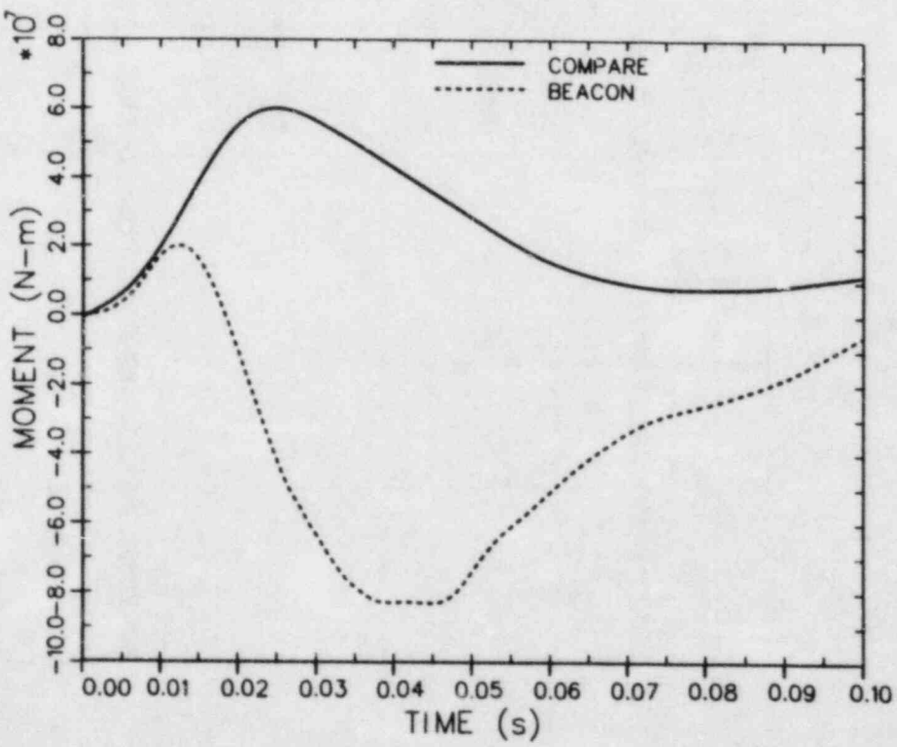

Fig. 4(b).
Comparison of COMPARE- and BEACON-calculated y-moments for Geometry 1.

for the force-moment surface areas composing the reactor cavity annulus. The force-moment surface noding used in the BEACON force-moment calculations is shown in Fig. 5.

In this discussion, the force-moment surface areas between 0 and 90° (Fig. 5) will be referred to as the left region. The left region is composed of force-moment surfaces 1, 3, 9, 11, 13, 15, 17, 19, 21, and 23. The areas occupying the 90--180° segment will be referred to as the right region. The right region is composed of force-moment surfaces 5, 7, 25, 27, 29, 31, 33, and 35. The coordinate system chosen for the force-moment surface is such that when the left region pressure build-up is greater than the pressure build-up in the right region, the result is a net negative x-direction force. Conversely, a net right region pressure build-up will result in a net positive x-direction force. This coordinate system also was used to obtain the COMPARE results.

The COMPARE base-case force results indicate a rapid pressure build-up in the region around the blowdown location that produced the net negative x-force until 0.015 s. As the steam was dispersed around the annulus, pressure contributions from the right region reversed the slope of the force curve. This trend continued until 0.07 s.

The BEACON x-force results indicate a trend similar to the COMPARE results until 0.01 s. Between 0.01 s and 0.015 s, the pressurization of the right region produced positive forces that reversed the slope of the force profile. The right region pressure contributions continued to dominate until 0.05 s.

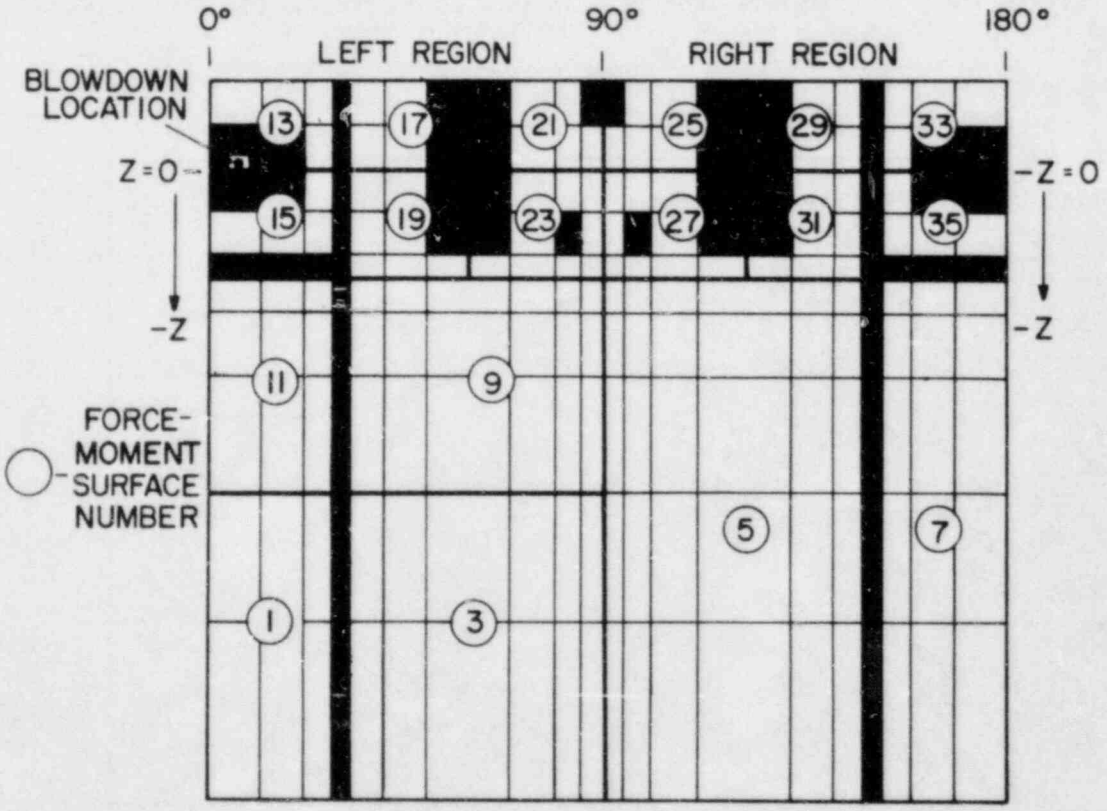

Fig. 5.
BEACON force-moment surface areas for Geometry 1.

To verify the differences in the force results, we made COMPARE and BEACON pressure comparisons for several force-moment surfaces at 0.025 s into the transient. (See Table II.) The pressures shown for force-moment surfaces 5, 7, 9, 11, 17, and 19 indicate the differences in the COMPARE- and BEACON-calculated pressure fields and correspondingly the differences in the force profiles. Force-moment surfaces 5 and 7 are located in the right region and are far removed from the blowdown location. Force-moment surfaces 11, 17, and 19 are located in the left region and are near the blowdown location. The BEACON-calculated pressures were 1.2 and 5.26 times higher than corresponding COMPARE values in fluid volumes corresponding to force-moment surface areas 5 and 7, respectively. The COMPARE-calculated pressures for areas 9, 11, 17, and 19 were 3.17, 2.53, 1.44, and 5.50 times higher than the equivalent BEACON pressures.

Even though the COMPARE and BEACON y-moments (Fig. 4b) are very different, the y-moment results are consistent with the force results. The pressure build-up in the COMPARE base case is concentrated in the left region below the $z = 0$ plane, resulting in net negative x-forces and net positive y-moment values. A net negative x-force and a negative z-moment arm produce net positive y-moments throughout the transient. In the BEACON calculation, the major pressure build-up is concentrated around the blowdown location in the left region early in the transient, quickly advances to the right region, and becomes dominant in the lower right region between 0.02 s and 0.05 s. The locally large positive force coupled with a negative z-moment arm results in the net negative y-moment calculated.

The difference in the COMPARE and BEACON annulus pressure distributions and resulting force-moment differences can be attributed to the basic assumptions inherent in each code. COMPARE calculates a one-dimensional flow field that is homogenous and in equilibrium. BEACON calculates a multidimensional, two-phase, nonhomogenous, and nonequilibrium field. These modeling assumptions

TABLE II

COMPARISON OF COMPARE- AND BEACON-CALCULATED FORCE-MOMENT SURFACE AREA PRESSURES FOR GEOMETRY 1 AT TIME = 0.025 s

Force-Moment Surface Area No.	COMPARE Pressure[a]	BEACON Pressure[a]
5	3.08×10^5	3.73×10^5
7	1.80×10^5	9.47×10^5
9	7.01×10^5	2.21×10^5
11	12.42×10^5	4.91×10^5
17	11.85×10^5	8.24×10^5
19	5.50×10^5	1.00×10^5

[a]Pressure in Newtons per square meter

relative to a steam/liquid blowdown are extremely different and do affect the pressure and resultant force-moment calculations. COMPARE's equilibrium assumption requires that the liquid water, steam, and air in a node have the same temperature and pressure. For a liquid blowdown, this results in a more rapid rate of liquid water flashing to steam than occurs in reality. Also, this is probably why COMPARE predicts higher pressures near the break than those measured and calculated by BEACON for the Battelle-Frankfurt C-Series tests.[6,9] The assumption caused the gradual pressurization of the left region near the blowdown location, which sustained the net negative x-forces and net positive y-moments. BEACON fluid thermodynamic assumptions permit the blowdown to flash to steam at a rate dependent on the surrounding conditions. This assumption allowed a significant amount of liquid to reach the right region, flash to steam, and produce the pressure distribution responsible for the BEACON force-moment results. An evaluation of the equilibrium assumptions and their effects on the force-moment calculations for this particular reactor cavity geometry is presented in Sec. III.

2. Geometry 2 Force-Moment Results. Figures 6(a) and 6(b) present the BEACON and COMPARE base-case geometry force and moment results. COMPARE calculated a maximum x-direction force of -1.70 MN at 0.052 s and a maximum moment about the y-axis of 1.01 MN-m at 0.02 s. BEACON calculated a maximum x-force of -4.75 MN between 0.05 s and 0.055 s, and a maximum y-moment of 1.58 MN-m between 0.02 s and 0.025 s.

As was the case for Geometry 1, the significant difference between the COMPARE and BEACON force-moment results for Geometry 2 can be attributed to the differences in the calculated pressure distributions for the force-moment surface areas composing the reactor cavity annulus. The force-moment surface noding used in the Geometry 2 BEACON force-moment calculation is shown in Fig. 7.

The coordinate system chosen for the Geometry 2 force-moment surface areas is identical to the coordinate system chosen for Geometry 1 (Sec. II.B.1). That is, net-negative x-forces will result if the left-region pressure build-up is greater than the right-region pressure build-up. Conversely, a net right-region pressure build-up will result in net-positive x-forces. The COMPARE results were obtained using the same coordinate system.

The COMPARE base-case force results indicate a rapid pressure build-up around the blowdown location that produces a net-negative x-force. For this geometry, a significant portion of the blowdown never advanced to the right region of the reactor cavity annulus. Consequently, the resultant force was always negative, with the maximum force (-1.70 MN) occurring at 0.05 s. The BEACON x-force results indicate trends similar to the COMPARE results. The calculated resultant x-force remained negative throughout the transient, with the maximum x-force (~-4.75 MN) occurring between 0.05 s and 0.055 s.

Differences between BEACON and COMPARE base-case pressure fields (x-forces) can be attributed partially to the amount of blowdown (mass) introduced to the reactor cavity annulus. The BEACON shield-wall penetration model calculated significantly larger liquid and steam (especially liquid) mass flows to the annulus than did the COMPARE calculation. The addition of significantly more liquid to the annulus in the BEACON calculation resulted in more liquid being flashed to steam, which produced greater pressures and correspondingly larger x-forces. Table III is a comparison of several of the BEACON and COMPARE base-case liquid and steam mass flow rates vs time. The BEACON shield-wall penetration model calculated liquid mass flow rates entering the annulus that were ~1.7 times larger than those the COMPARE model calculated at corresponding times.

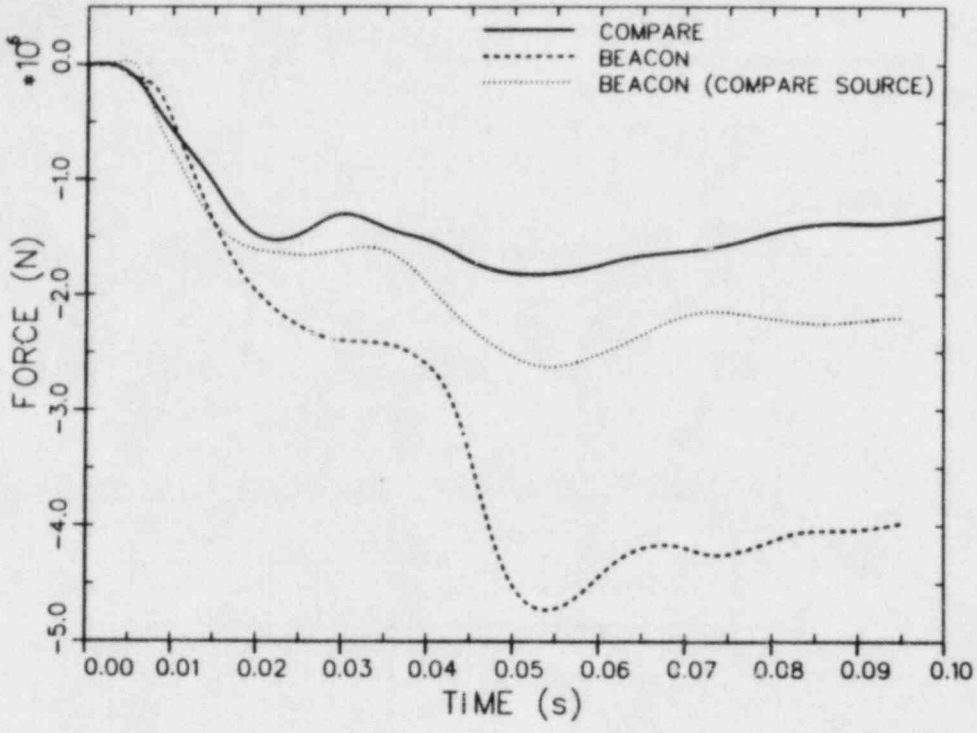

Fig. 6(a).
Comparison of COMPARE and BEACON calculated x-forces for Geometry 2.

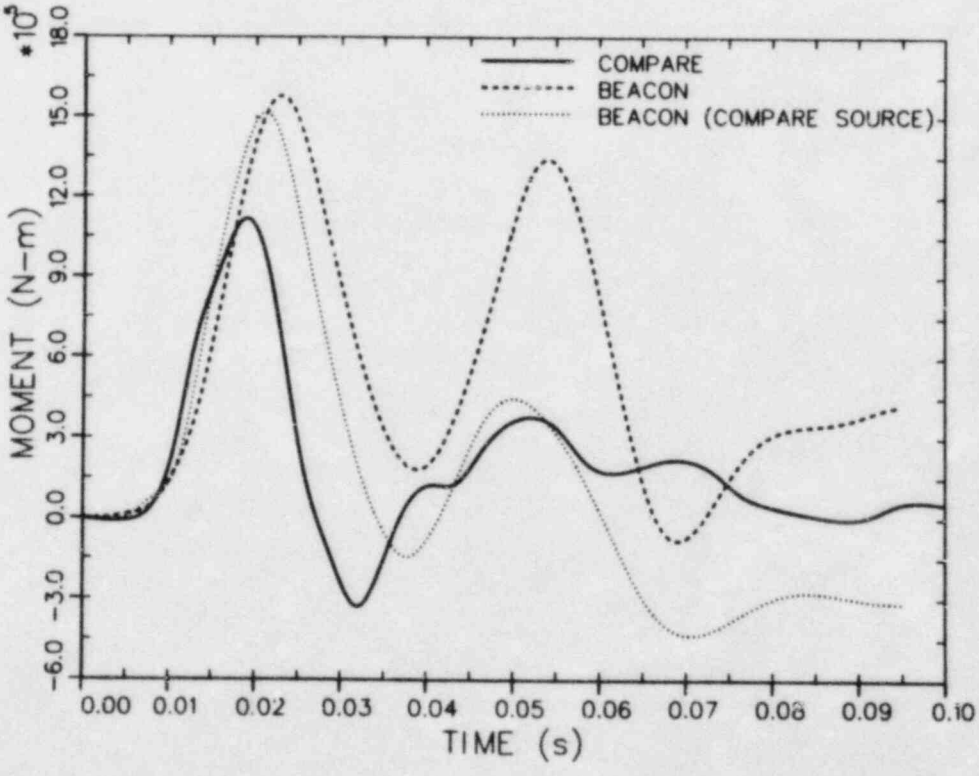

Fig. 6(b).
Comparison of COMPARE and BEACON calculated y-moments for Geometry 2.

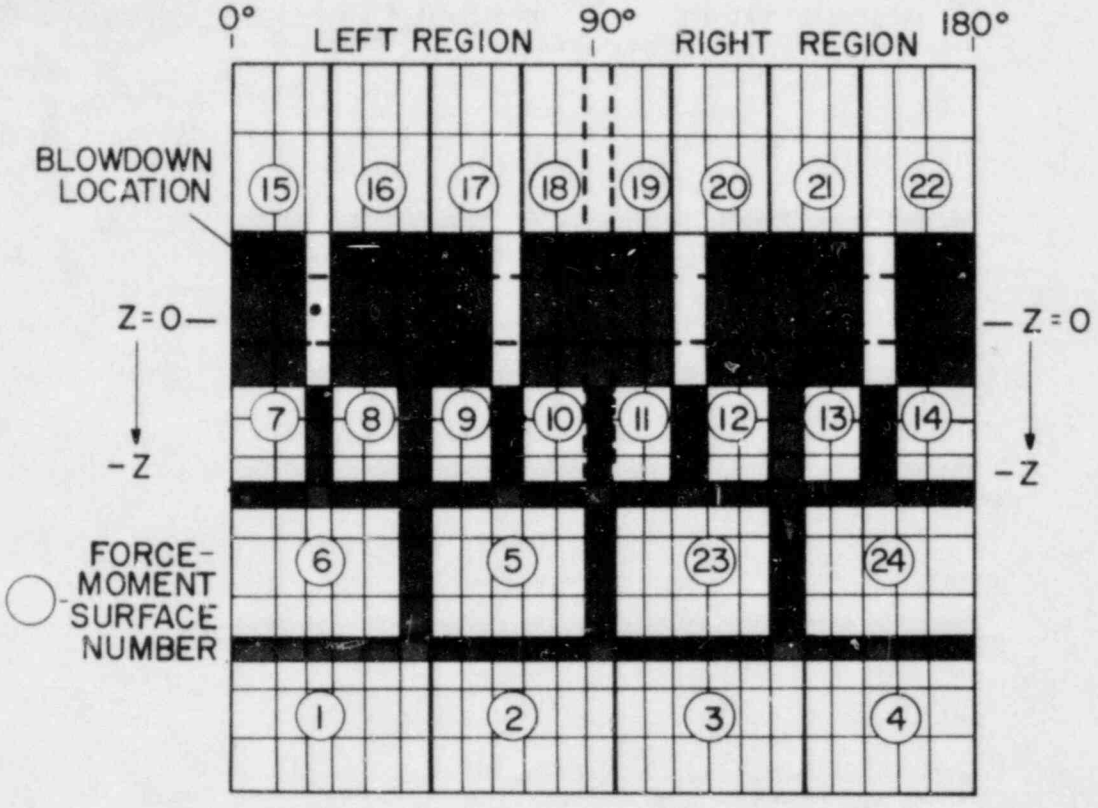

Fig. 7.
BEACON force-moment surface areas for Geometry 2.

TABLE III

COMPARISON OF COMPARE AND BEACON BASE-CASE
BLOWDOWN MASS FLOW RATES VS TIME

Time (s)	COMPARE Liquid Mass Flow (kg/s)	COMPARE Steam Mass Flow (kg/s)	BEACON Liquid Mass Flow (kg/s)	BEACON Steam Mass Flow (kg/s)
0.005	40.41	22.51	36.81	25.52
0.01	131.83	49.74	264.45	72.98
0.02	266.97	76.11	544.66	94.87
0.03	337.96	84.19	662.32	87.39
0.04	393.07	89.87	705.56	73.38
0.05	426.65	92.68	721.08	71.36
0.06	434.58	92.88	726.50	65.71
0.07	425.56	91.34	725.58	61.37
0.08	414.10	90.04	719.61	58.03
0.09	409.77	89.39	712.16	55.44

Tables IV and V present a comparison of the BEACON and COMPARE base-case calculated force-moment area pressures at 0.02 s and 0.05 s. BEACON blowdown location pressures* were calculated to be ~1.53 times larger at ~0.025 s and ~2.47 times larger at ~0.05 s than the corresponding COMPARE-calculated pressures at these times.

The y-moment results for the COMPARE calculation reveal that the pressure build-up near or around the blowdown location is concentrated below the z = 0 plane in the left region of the annulus mesh, with the maximum y-moment (1.01 MN-m) occurring at 0.02 s. The y-moment occurring between ~0.05 s and ~0.055 s corresponds to the maximum calculated x-force. The maximum x-force does not produce the maximum y-moment because of the pressurization of the right-region volumes connecting the annulus to the upper containment. These volumes correspond to BEACON force-moment surface areas 19 through 22.

The BEACON y-moment results indicate the initial pressurization of the annulus around the blowdown location, which results in the maximum moment (~1.58 MN-m) between 0.02 s and 0.025 s. An ~1.35 MN-m y-moment, corresponding to the maximum x-force, was calculated at ~0.055 s. The calculated y-moment at ~0.055 s is more prominent than the COMPARE-calculated moment at this time because of the substantially larger liquid mass flows calculated to enter the annulus and the lack of pressurization of the force-moment surface areas (19 through 22) connecting the right region of the annulus to the upper containment. The upper containment was represented by a constant pressure boundary in the BEACON model.

The uncertainty associated with the shield-wall penetration geometry coupled with the BEACON shield-wall penetration model's calculated annulus mass flow rates indicated that a second BEACON reactor cavity calculation should be performed using the COMPARE base-case calculated annulus mass flows and enthalpy vs time as the BEACON source input. The results** of this calculation are presented in Figs. 6(a) and 6(b), respectively. This BEACON calculation shows good agreement with the COMPARE base-case results until ~0.035 s. The maximum x-force was calculated to be ~-2.5 MN at ~0.055 s. This is substantially larger than the COMPARE maximum x-force of -1.70 MN, which occurred at approximately the same time. The moment profiles reflect the differences in the calculated x-forces after ~0.35 s.

Because the blowdown mass flow and enthalpy vs time were identical and the BEACON cells composing the COMPARE base-case volumes agree quite well in terms of fluid volume and flow area, the difference between the two calculations can be attributed to the internal differences between the two codes (Sec. II.B.1). Multidimensional effects are important for this particular geometry. As discussed in Sec. II.A.2, the hot-leg and cold-leg pipes were modeled as a combination of obstacle cells and partially blocked fluid cells. The source (blowdown) was positioned at the z = 0 plane between two of the primary system pipes. (See Appendix A, Fig. A-5.) The source location resulted in a liquid and vapor velocity field predominately in the $\pm$ y direction. Figures 8(a) and 8(b) show the liquid velocity field at 0.02 s and 0.05 s for the BEACON (COMPARE SOURCE) calculation. As a result of the BEACON-calculated velocity field, portions of the right region of the BEACON reactor cavity annulus mesh (Fig. 7) were not pressurized by flashing liquid as calculated in the COMPARE base case. The lack of right-region pressure contributions in the BEACON calculations resulted in the

*Arithmetic average of force-moment surface area 7 and 15 pressures.
**BEACON (COMPARE SOURCE)

TABLE IV

COMPARISON OF COMPARE- AND BEACON-CALCULATED FORCE-MOMENT SURFACE AREA PRESSURES FOR GEOMETRY 2 AT TIME ~0.02 s

Force-Moment Surface Area No.	COMPARE Base-Case Pressure[a]	BEACON Base-Case Pressure[a]	BEACON (COMPARE SOURCE) Pressure[a]
1	1.29×10^5	1.35×10^5	1.44×10^5
2	1.17×10^5	1.17×10^5	1.22×10^5
3	1.08×10^5	1.05×10^5	1.04×10^5
4	1.03×10^5	1.01×10^5	1.01×10^5
5	1.41×10^5	1.26×10^5	1.28×10^5
6	1.51×10^5	1.44×10^5	1.41×10^5
7	1.78×10^5	2.92×10^5	2.50×10^5
8	1.67×10^5	2.25×10^5	2.00×10^5
9	1.50×10^5	1.14×10^5	1.13×10^5
10	1.45×10^5	1.15×10^5	1.12×10^5
11	1.19×10^5	1.12×10^5	1.14×10^5
12	1.19×10^5	1.07×10^5	1.08×10^5
13	1.05×10^5	1.03×10^5	1.02×10^5
14	1.05×10^5	1.01×10^5	1.01×10^5
15	1.64×10^5	2.32×10^5	1.49×10^5
16	1.52×10^5	1.86×10^5	1.65×10^5
17	1.38×10^5	1.06×10^5	1.04×10^5
18	1.38×10^5	1.07×10^5	1.05×10^5
19	1.28×10^5	1.07×10^5	1.09×10^5
20	1.28×10^5	1.04×10^5	1.07×10^5
21	1.21×10^5	1.03×10^5	1.02×10^5
22	1.21×10^5	1.01×10^5	1.01×10^5
23	1.16×10^5	1.10×10^5	1.12×10^5
24	1.05×10^5	1.02×10^5	1.01×10^5

[a] Pressure is in Newtons per square meter.

TABLE V

COMPARISON OF COMPARE- AND BEACON-CALCULATED FORCE-MOMENT SURFACE AREA PRESSURES FOR GEOMETRY 2 AT TIME ~0.05 s

Force-Moment Surface Area No.	COMPARE Base-Case Pressure[a]	BEACON Base-Case Pressure[a]	BEACON (COMPARE SOURCE) Pressure[a]
1	1.30×10^5	1.31×10^5	1.23×10^5
2	1.27×10^5	1.33×10^5	1.22×10^5
3	1.22×10^5	1.24×10^5	1.14×10^5
4	1.14×10^5	1.30×10^5	1.21×10^5
5	1.35×10^5	1.04×10^5	0.91×10^5
6	1.48×10^5	1.33×10^5	1.00×10^5
7	2.25×10^5	6.10×10^5	3.91×10^5
8	2.20×10^5	4.67×10^5	3.19×10^5
9	1.52×10^5	1.24×10^5	1.12×10^5
10	1.48×10^5	1.02×10^5	0.97×10^5
11	1.31×10^5	1.00×10^5	0.97×10^5
12	1.31×10^5	1.00×10^5	0.98×10^5
13	1.22×10^5	1.04×10^5	1.02×10^5
14	1.22×10^5	1.06×10^5	1.02×10^5
15	2.05×10^5	4.54×10^5	2.49×10^5
16	2.00×10^5	3.59×10^5	2.55×10^5
17	1.55×10^5	1.20×10^5	1.14×10^5
18	1.44×10^5	1.06×10^5	1.05×10^5
19	1.28×10^5	1.02×10^5	1.02×10^5
20	1.28×10^5	1.02×10^5	1.02×10^5
21	1.21×10^5	1.02×10^5	1.02×10^5
22	1.21×10^5	1.05×10^5	1.03×10^5
23	1.27×10^5	1.04×10^5	0.97×10^5
24	1.18×10^5	1.12×10^5	1.06×10^5

[a] Pressure is in Newtons per square meter.

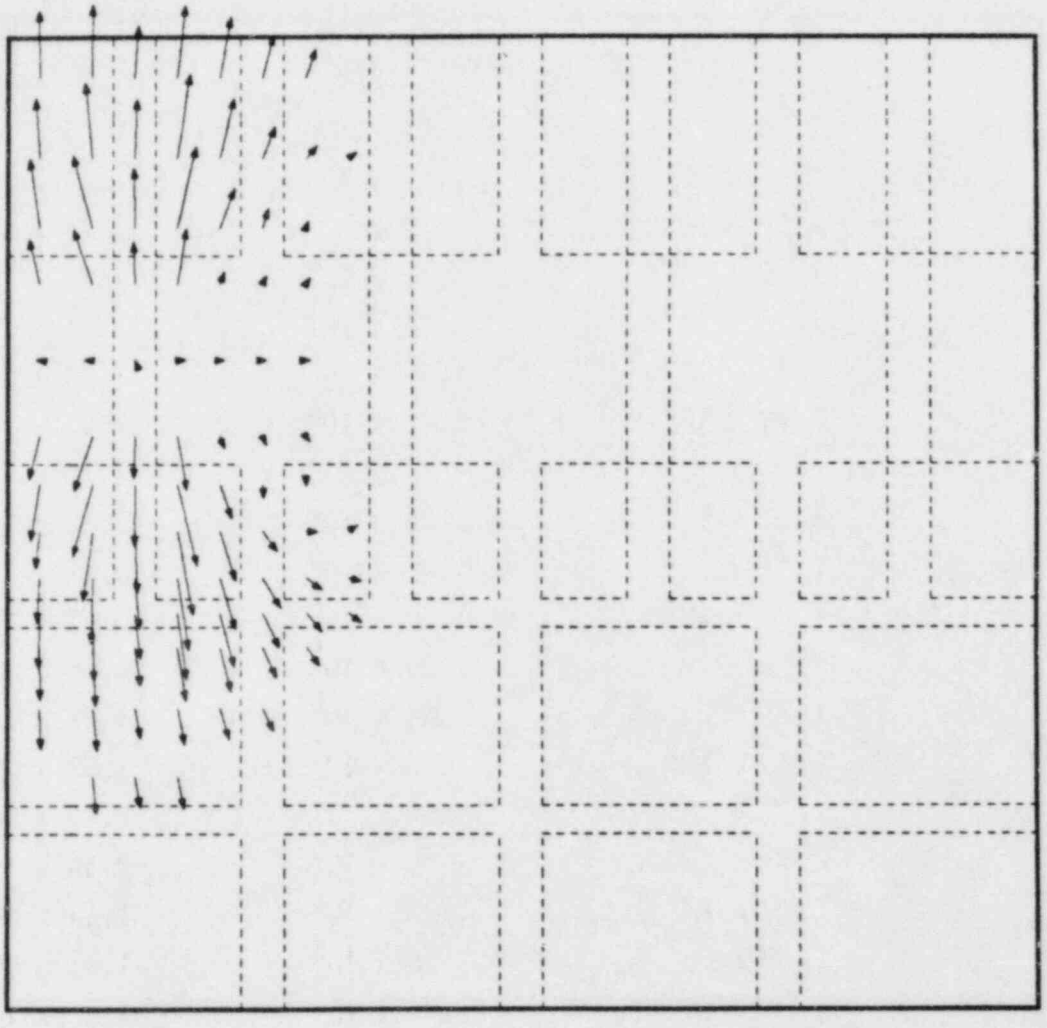

Fig. 8(a).
BEACON-calculated liquid velocity field at 0.02 s for Geometry 2.

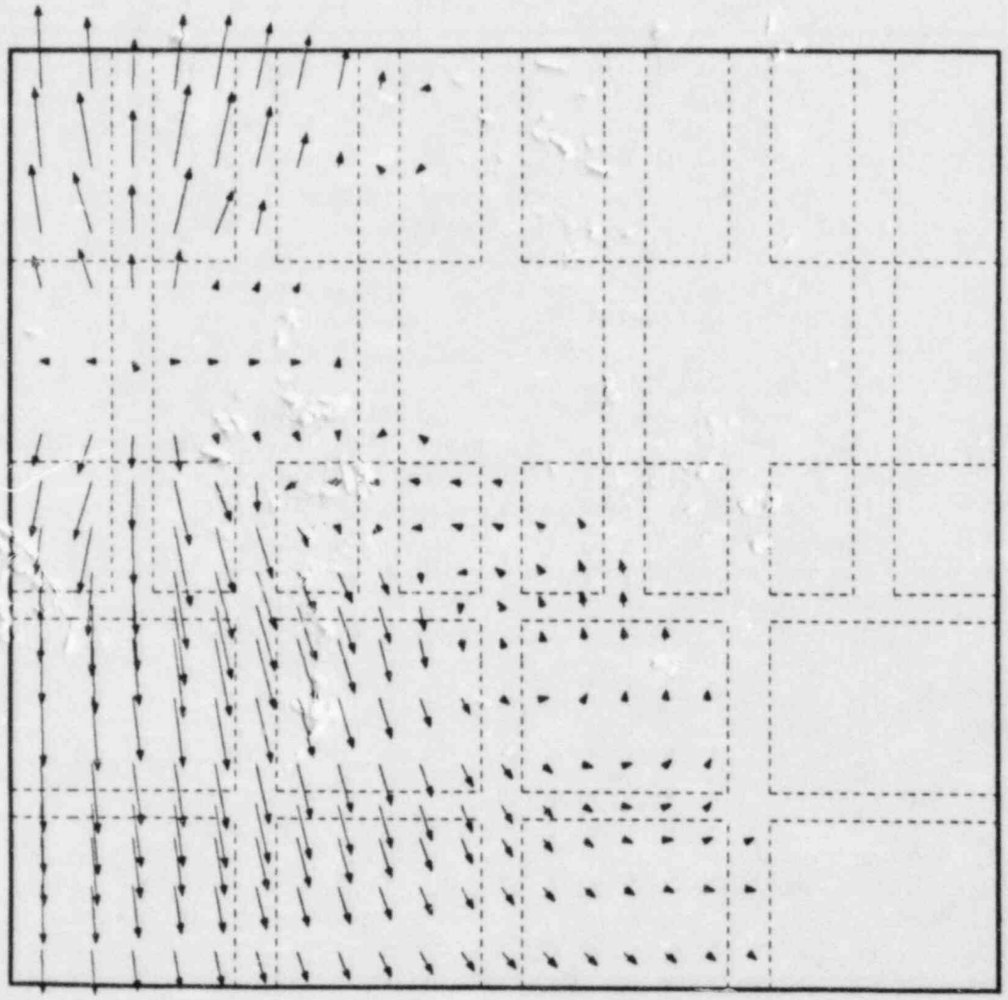

Fig. 8(b).
BEACON-calculated liquid velocity field at 0.05 s for Geometry 2.

larger x-forces (relative to the COMPARE calculation) after ~0.035 s. A comparison of the BEACON (COMPARE SOURCE) and the COMPARE base-case force-moment area pressures is shown in Tables IV and V.

Further analysis of the BEACON (COMPARE SOURCE) force-moment results indicates that a blowdown modeling scheme that distributes the source around the perimeter of the broken cold-leg should be investigated. Specifically, the location of the blowdown in one fluid cell at the z = 0 plane resulted in liquid and vapor velocity field development primarily in the $\pm$y direction. As a result, the right region of the unwrapped annulus was not pressurized by flashing liquid, which contributed to the larger calculated x-forces. The restriction of x-direction velocity field development resulting from the single-cell (z = 0 plane) blowdown location may be an inaccurate representation of the flow entering the reactor cavity from the shield-wall penetration. If a cold-leg break were to occur in the shield-wall penetration, an annular multiphase flow field would develop along the broken pipe. As the portion of the flow moving toward the reactor enters the reactor cavity annulus, it would impact the vessel and be dispersed away from the broken cold-leg in the radial direction. In the BEACON reactor cavity annulus mesh, the radial dispersion (velocity components in both directions) possibly would be modeled more accurately by placing the source in several fluid cells representing the perimeter of the broken cold-leg.

If a multiple blowdown location modeling scheme were implemented, BEACON might calculate more liquid transport to the reactor cavity annulus right region and a smaller average blowdown region pressure. This could produce a lower (in terms of magnitude) maximum x-force. The significance of a multiple blowdown model can be determined only by performing additional BEACON calculations. Other BEACON modeling assumptions should be investigated also (for example, the effect of the pipe curvature).

3. Summary of the Geometry 1 and 2 Force-Moment Results. The differences in the COMPARE and BEACON annulus pressure distributions and resulting force-moment differences for the base-case calculations can be attributed to the basic assumptions (homogenous vs nonhomogenous, equilibrium vs nonequilibrium, and one-dimensional vs multidimensional) of each code. In Geometry 1, the chemical nonequilibrium (flashing) modeling in BEACON allowed a substantial amount of liquid to reach the right region of the annulus and flash to steam, thereby producing a different x-force and y-moment profile. For Geometry 2, the shield-wall penetration model calculated significantly larger mass flows to the annulus relative to the COMPARE calculation. The addition of more liquid into the annulus produced higher pressures and correspondingly larger x-forces and y-moments. The second BEACON calculation, using the COMPARE base-case mass flows and enthalpy, produced different x-force results after ~0.035 s as a result of the interaction between the blowdown and the particular multidimensional modeling present in BEACON. If a multiple blowdown location modeling scheme (Sec. II.2) were implemented for the Geometry 2 reactor cavity annulus, BEACON may calculate a lower peak x-force and y-moment, which may produce better agreement with the COMPARE-calculated results. The significance of a multiple blowdown location model can be determined only by performing additional BEACON calculations.

III. EVALUATION OF THE DIFFERENCES IN CALCULATED FORCES AND MOMENTS BETWEEN BEACON AND COMPARE FOR REACTOR CAVITY SUBCOMPARTMENT ANALYSES

As shown in the previous section, significant differences do exist between BEACON- and COMPARE-calculated forces and moments. These differences are

attributed to the simplifying assumptions, primarily the equilibrium assumptions, made in the COMPARE code. Multidimensional effects also are important as shown in the previous section. COMPARE does not account for mechanical (momentum transfer), chemical (mass transfer), or thermal (energy transfer) nonequilibrium between phases. The BEACON code does not arbitrarily assume equilibrium. BEACON provides for coupling between the gas and liquid fields through interphasic exchange functions included in the continuity, momentum, and energy equations for the two fields. These functions model the effects of mass, momentum, and energy transfer. The degree of coupling depends on the interphasic model and the associated parameteric values used. The resulting fluid computations may be either equilibrium or nonequilibrium.

The BEACON user may select either user-defined (USERDEF option) or best-estimate (BEST option) interphasic models. User-defined models are intended for special applications and do not account for the presence of an inert gas. The best-estimate models do account for the presence of an inert or noncondensible gas and are physically realistic for containment flow situations. When using BEACON with the BEST option, all parametric values governing the degree of coupling (equilibrium) between phases are set internally in the code. To handle the special flow situation where rapid flashing occurs (as in a high-pressure liquid break), a modeling switch is incorporated in BEACON when in the best-estimate computation mode. The modeling switch allows the best-estimate exchange functions to be used for dispersed droplet flow regimes but allows the Rivard-Torrey[10] mass transfer model (a user-defined model) to be used for flashing flow regimes. The switch to the Rivard-Torrey model is based on the degree of superheat present in the liquid field.[4] Details of the interphasic exchange models can be found in Ref. 4.

A. Effects of Equilibrium Assumptions on BEACON- and COMPARE-Calculated Forces and Moments

Equilibrium effects on calculated forces and moments were evaluated by modifying the BEACON code to run in the best-estimate mode and allowing the user to vary the internally set parametric values governing the degree of interphasic equilibrium in the calculations. Our approach was to evaluate the three equilibrium effects (mechanical, thermal, and chemical) separately. This was done by varying the parameter value governing one equilibrium effect while using the normal best-estimate values for the other two effects. In this manner, an assessment could be made concerning the degree of influence that each equilibrium effect has on calculated forces and moments for blowdowns within reactor cavity geometries. We performed the following calculations for Geometry 1 (described in Sec. II).

1. Mechanical Equilibrium Effects. Momentum transfer between phases in the BEACON code is the product of a momentum exchange coefficient K and the velocity vector difference between the gas and liquid phases. K is calculated by the best-estimate interphasic momentum transfer model and is primarily a function of the droplet size distribution. If the calculated K value falls below a minimum value set internally in the code, the minimum value is used. The minimum K value is a limit imposed by best-estimate correlations and numerical stability considerations. The best-estimate minimum K value is 10^7 and generally results in near mechanical equilibrium.

Initial efforts focused on investigating the effects of the droplet size distribution (controlled by the critical Weber number) on the calculated K value which in turn affect the calculated forces and moments. Varying the Weber number to vary drop size distribution always resulted in K values less than 10^5, a minimum value established in this study below which the calculations would

become unstable. Therefore, varying the drop size distribution had no effect other than to force the code to use the minimum K value. Nevertheless, the variation of 2 orders of magnitude in the minimum K value (10^5 and 10^7) allowed for enough variation in mechanical equilibrium to assess its importance on BEACON-calculated forces and moments for blowdowns within reactor cavities.

Figures 9(a) and 9(b) show the effects of using the two different minimum K values on the BEACON-calculated forces and moments. Using the 10^5 value increases the degree of mechanical nonequilibrium between the phases (that is, unequal velocities) with the result that flashing and subsequent pressure build-up occur closer to the break. This in turn reduces the peak force and moment as shown. Although the momentum exchange coefficient was varied by 2 orders of magnitude, the effect on the reduction of the peak calculated force and moment was only about 6 . Therefore, it is concluded that mechanical nonequilibrium effects have a minor effect on BEACON-calculated forces and moments for this type of geometry.

2. Thermal Equilibrium Effects. The energy transfer between phases in BEACON is handled similarly to the momentum transfer. Specifically, the energy exchange is a product of an interfacial heat transfer exchange coefficient, R, and the temperature difference between the gas and liquid phases. Higher R values result in a greater degree of thermal equilibrium than lower R values. Also, a minimum value of 10^7 is used for calculative stability purposes (that is, the code will not execute for R values less than 10^7). Because the interphasic energy transfer model generally calculates values less than this, the minimum value is used exclusively in the best-estimate computation mode for dispersed droplet flow regions. However, an R value of 10^7 generally results in some degree of thermal nonequilibrium. For flashing flow regions, a value of 10^{10} always is used.

To evaluate the effects of variations in thermal equilibrium, BEACON forces and moments for Geometry 1 were recomputed using a minimum R value of 10^{10}, an increase of 3 orders of magnitude from the best-estimate value. This change increased the degree of thermal equilibrium between phases but had little effect on the forces and moments relative to the best-estimate case ($R = 10^7$). The effects on forces and moments are shown in Figs. 10(a) and 10(b). The negligible effect on the forces and moments is because flashing occurs over a wide area of the model for both cases, and as a result, an R value of 10^{10} is being used in these regions for both cases. Thermal nonequilibrium effects are dominated by the flashing phenomena and therefore have little influence on BEACON-calculated forces and moments.

3. Chemical Equilibrium Effects. Inspection of the BEACON calculations in Sec. II for Geometry 1 shows that the predominant mechanism for mass transfer (liquid to vapor) throughout the model is that of a flashing liquid. As mentioned at the beginning of this section, BEACON uses the Rivard-Torrey mass transfer model for flashing flows. This model calculates the evaporation (flashing) rate, J_e, with the following relationship.

$$J_e = \lambda_e A \rho' \theta (T_S R_V)^{1/2} (T - T_S)/(3T_S), \text{ for } T \geq T_S ,$$

where

A = interfacial surface area between the two phases per unit volume (M^2/M^3),

J = mass transfer rate per unit volume (kg/m^3-s),

R_v = gas constant = $463.4 \left(\frac{J}{kg\ K}\right)$,

T = temperature,

θ = void fraction,

λ = rate multiplier, and

ρ' = macroscopic density, mass per unit volume (kg/m^3),

and subscripts

e = evaporation,

ℓ = liquid, and

s = saturation.

BEACON uses a nominal value for λ_e of 0.1 when using the above model for calculating the mass transfer rate in regions where flashing occurs. To assess the importance of flashing on the calculated forces and moments, λ_e was varied from 0.001 to 0.4. Lower values reduce the rate at which liquid is flashed to vapor, whereas higher values increase the rate. The λ_e value of 0.4 was a maximum limit above which the calculations became unstable. The effects of varying the flashing rate on calculated forces and moments for Geometry 1 are shown in Figs. 11(a) and 11(b). Forces and moments for λ_e = 0.1 correspond to those shown for Geometry 1 in Sec. II.

As shown in Figs. 11(a) and 11(b), the flashing rate has a significant effect on BEACON-calculated forces and moments. As the rate multiplier λ_e is reduced, the flashing rate is reduced. This in turn reduced both the rate of the pressure build-up and the overall forces and moments. Increasing λ_e from 0.1 to 0.4 resulted in a small decrease in the force and a small increase in the moment. The force reduction is a result of a slight difference in the overall pressure distribution. The increase in moment results from the higher pressure achieved because of the increase in flashing rate. These results show that the phenomena of a flashing fluid and the degree of flashing (that is, chemical nonequilibrium) plays an important role in determining the overall forces and moments for blowdowns within reactor cavities.

B. Effects of Turbulent Jet Diffusion on General Subcompartment Analyses

Containment subcompartment analysis problems involve calculating the differential pressure build-up between subcompartments resulting from a high-energy blowdown in one of the subcompartments. For some containment geometries, the subcompartments are interconnected by small-diameter orifices that provide a flow path for the blowdown to propagate through the containment system and equalize the pressure.

Because of the rapid pressure build-up in the subcompartment where the blowdown occurs, the interconnecting orifices initially will force the flow to jet from one subcompartment to another. If the computer code being used for this type of analysis does not account for turbulent jet diffusion effects, the codes' calculations may predict higher mass flow rates between some subcompartments (depending on the geometry) and would result in lower differential pressures than if turbulent jet diffusion effects were taken into consideration.

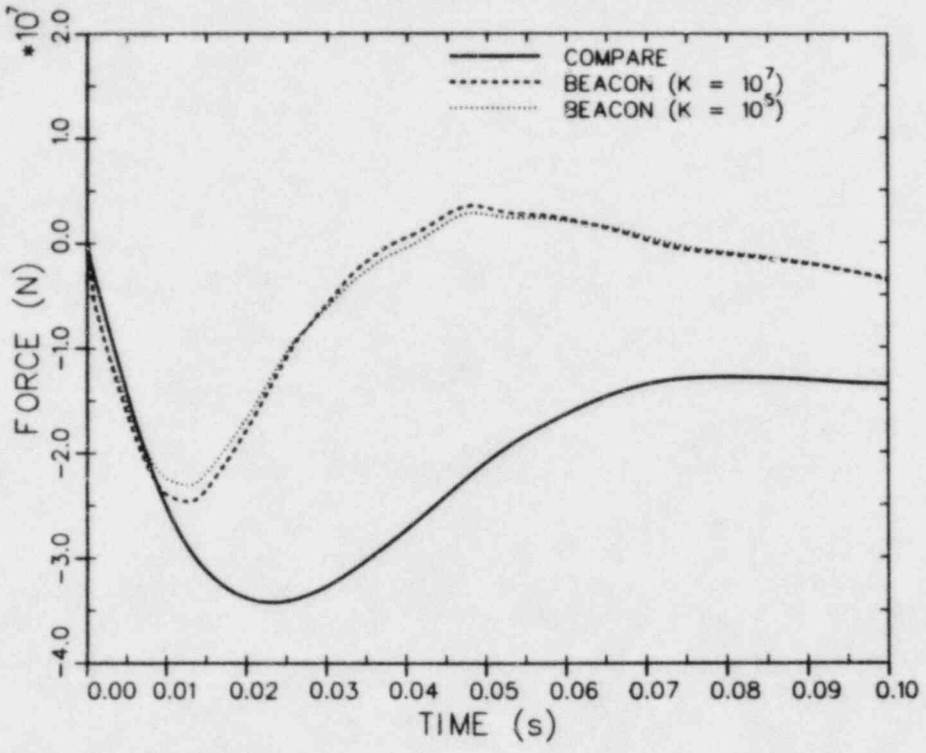

Fig. 9(a).
Effect of mechanical nonequilibrium on BEACON-calculated x-forces for Geometry 1.

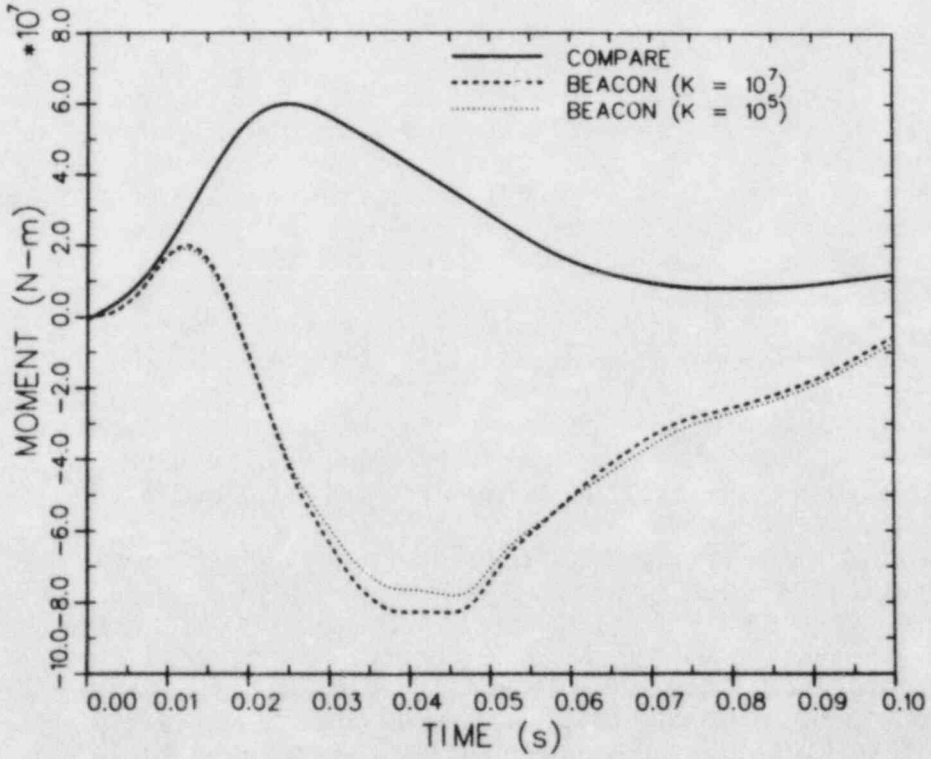

Fig. 9(b).
Effect of mechnical nonequilibrium on BEACON-calculated y-moments for Geometry 1.

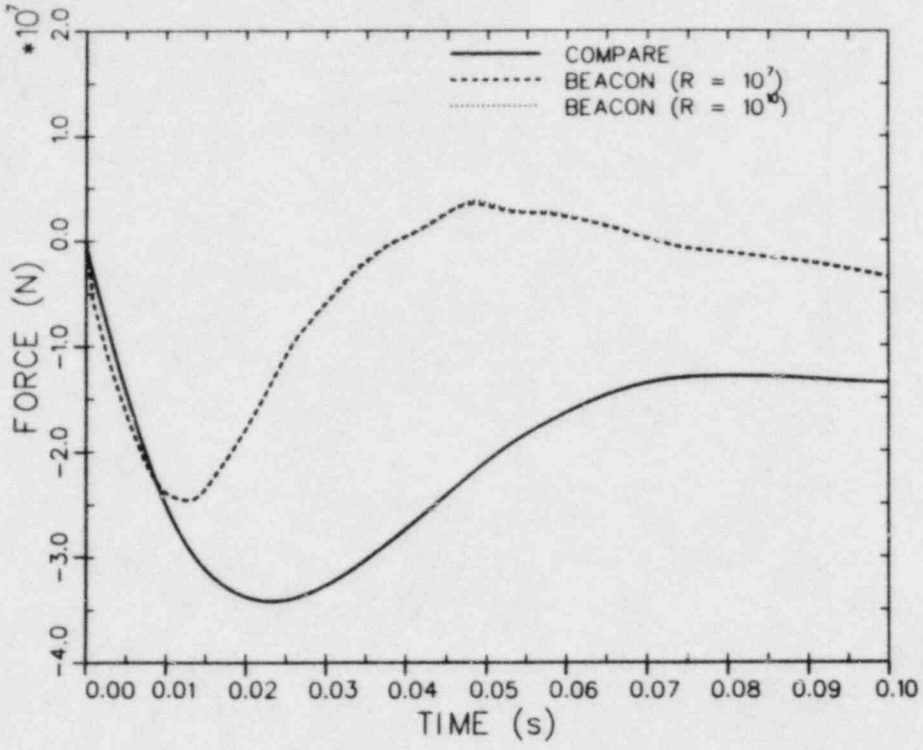

Fig. 10(a).
Effect of thermal nonequilibrium on BEACON-calculated x-forces for Geometry 1.

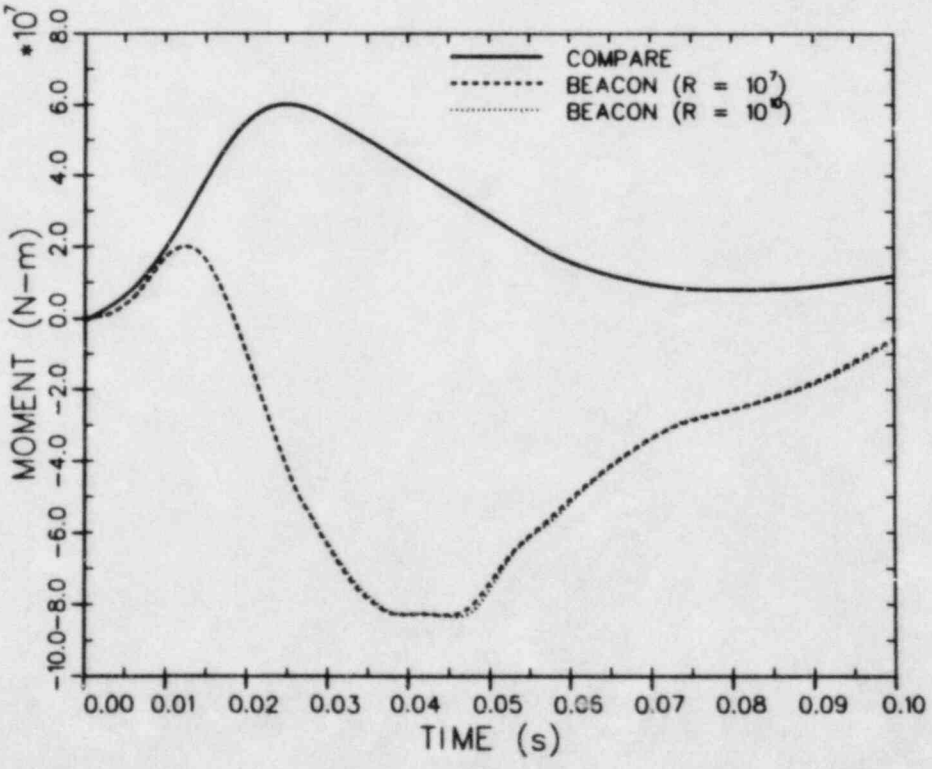

Fig. 10(b).
Effect of thermal nonequilibrium on BEACON-calculated y-moments for Geometry 1.

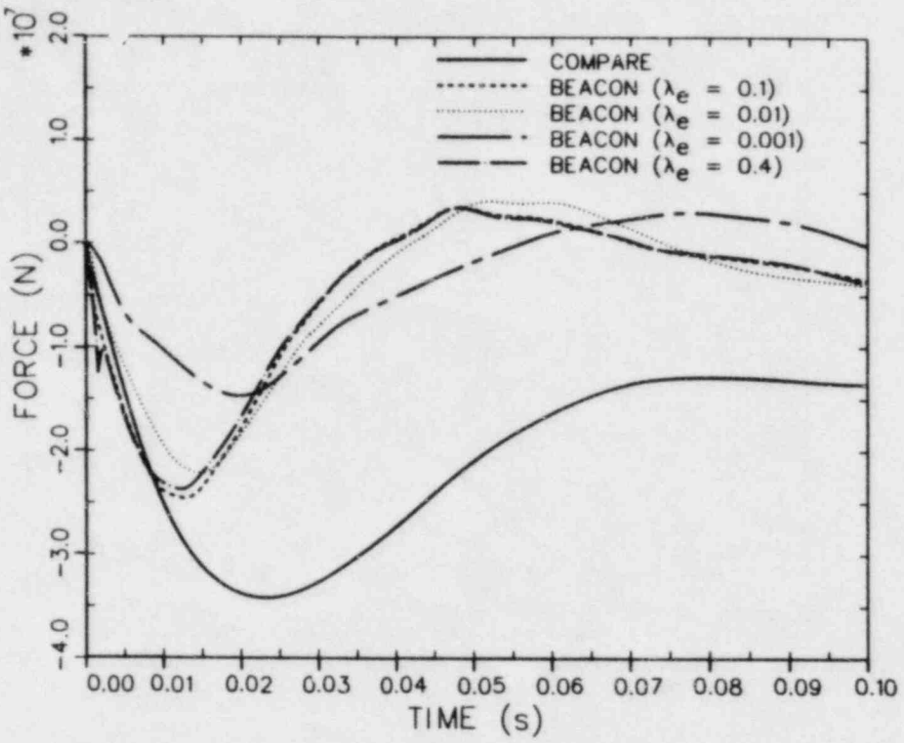

Fig. 11(a).
Effect of chemical nonequilibrium on BEACON-calculated x-forces for Geometry 1.

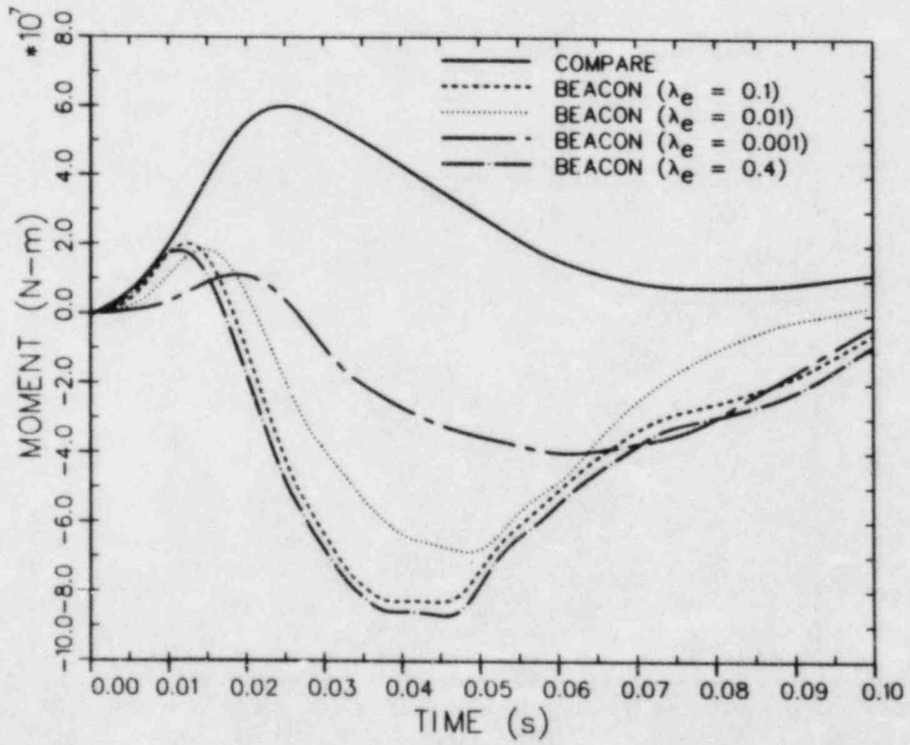

Fig. 11(b).
Effect of chemical nonequilibrium on BEACON-calculated y-moments for Geometry 1.

To verify the above hypothesis, we incorporated a simple turbulent jet diffusion model into the BEACON code to account for transverse turbulent momentum diffusion. A hypothetical problem then was calculated with both COMPARE and the modified BEACON code to evaluate the effects of turbulent jet momentum diffusion on mass flow rates between subcompartments. A brief description of the simple turbulent model incorporated into the BEACON code will be given. The accuracy of the model is assessed by comparing a BEACON calculation for a circular free turbulent jet with experimental data. The results of the hypothetical problem mentioned above are presented after this discussion.

1. Turbulent Jet Momentum Diffusion Model. The turbulent jet momentum diffusion model incorporated into the BEACON code is based on the following relationship.

$$\tau = \rho\epsilon_o \frac{\partial u}{\partial r} \quad ,$$

where

ϵ_o = turbulent eddy diffusivity coefficient,

$\frac{\partial u}{\partial r}$ = transverse velocity gradient,

ρ = density,

τ = shear stress,

u = velocity component in the axial direction, and

r = radial direction.

Experimental studies have established the following relationship for ϵ_o.

$$\epsilon_o = 0.0161\ \pi\ u_o r_o \quad ,$$

where

u_o = jet velocity at its source and

r_o = jet radius at its source.

The product $\rho\epsilon_o$ is analagous to the absolute viscosity coefficient that relates the shear stress to the transverse velocity gradient for laminar flow. Because BEACON employs a laminar viscous coefficient μ_L in its momentum diffusion modeling, the modification to include turbulent momentum diffusion effects was done as follows.

$$\mu = \mu_L + \mu_T \quad ,$$

where

μ = total absolute viscosity,

μ_L = normal BEACON laminar absolute viscosity, and

$\mu_T = \rho\epsilon_o$ = turbulent eddy viscosity.

To be technically correct, μ_T should be included only within the turbulent jet shear region. However, modification of the BEACON code to track the jet shear region was beyond the scope of this study. Therefore, the turbulent viscous terms are applied throughout the computational fluid region. To test the accuracy of the turbulent model, a BEACON model was developed to calculate the steady-state velocity profiles for a turbulent circular free jet of air with a source velocity of 46.3 m/s (u_o) and radius of 0.5 m (r_o). A more detailed description of the jet model and the input deck is presented in Appendix B. The calculated steady-state radial and axial velocity profiles were compared with the steady-state experimental data in Ref. 11.

Figure 12 presents a normalized transverse axial velocity profile comparison between the BEACON calculations and experimental data for a position three diameters downstream of the jet source. The normalized ordinate in the figure is the ratio of the axial velocity to the maximum (centerline) axial velocity, whereas the normalized abscissa is the ratio of the radial distance from the centerline to the radial distance where the axial velocity is one-half the maximum axial velocity. Two BEACON calculations are presented--one with just the laminar viscous terms included in the calculation and the other with the addition of the turbulent viscous terms. As shown, the laminar computations produce very little transverse diffusion of momentum. Addition of the turbulent viscous terms results in a significant amount of transverse momentum diffusion, and the agreement with experimental data is good considering the simplicity of the turbulent model. Velocity profile comparisons at a distance of 10 diameters downstream from the jet source are shown in Fig. 13. The laminar calculations are similar to those in the previous figure, and the turbulent calculations agree well with the experimental data.

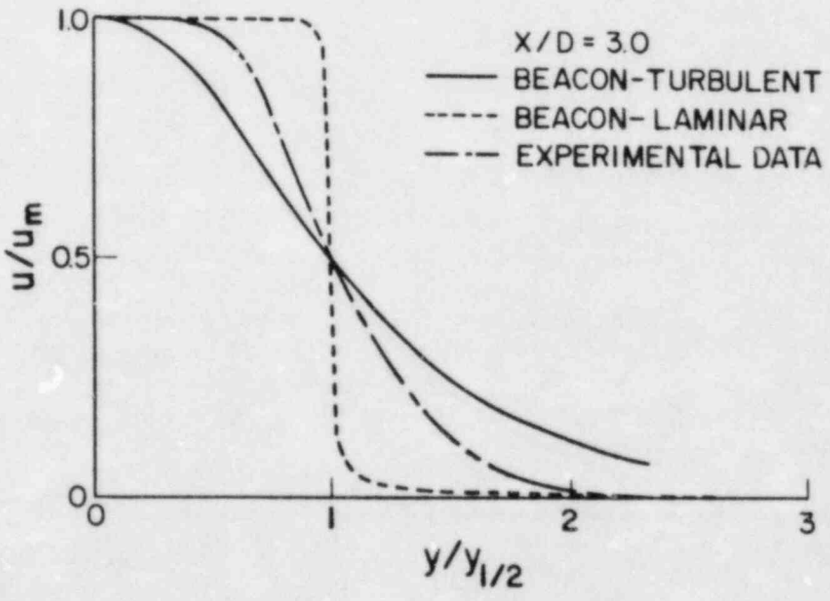

Fig. 12.
Comparisons of calculated transverse axial velocity profiles with experimental data.

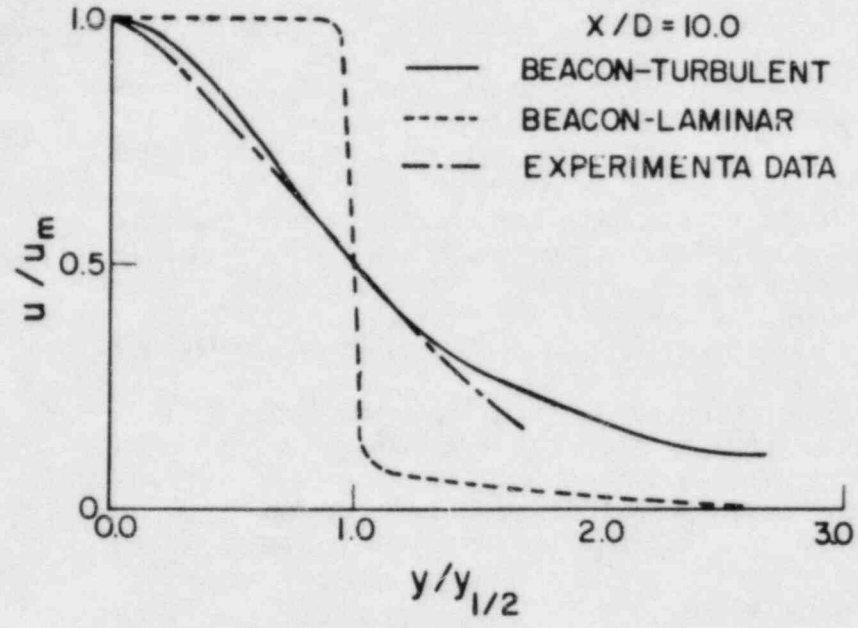

Fig. 13.
Comparisons of calculated transverse axial velocity profiles with experimental data.

The effects of the turbulent model on axial momentum diffusion are shown in Fig. 14. In this figure, the calculated normalized axial velocity profile is compared with the experimental data for both laminar and turbulent cases.

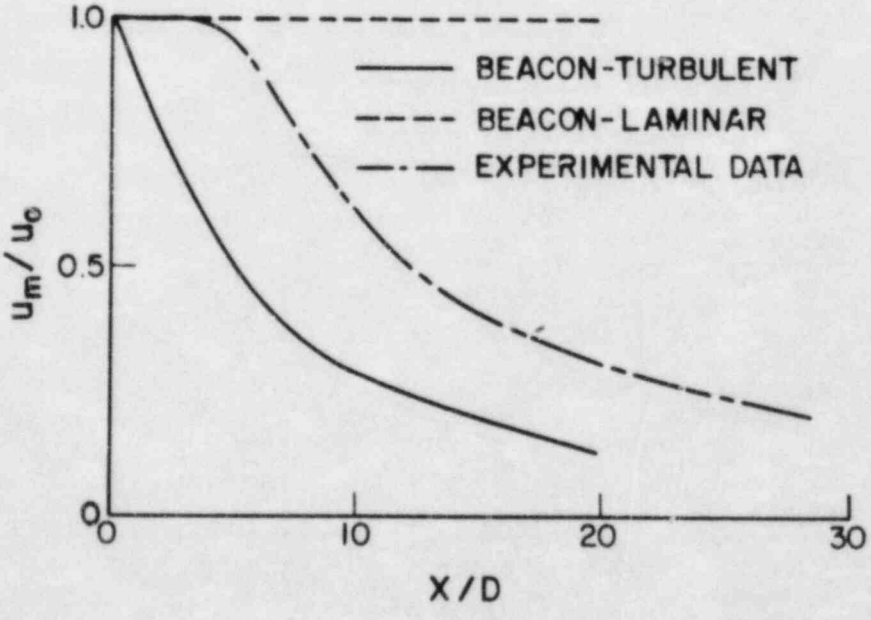

Fig. 14.
Comparison of calculated centerline axial velocity profiles with experimental data.

The normalized ordinate in this figure is the ratio of the maximum axial velocity to the velocity of the jet at its source. The abscissa represents the normalized distance downstream from the source (that is, the ratio of the downstream distance to the jet diameter at its source). As shown, the laminar viscous model results in no axial momentum diffusion, and the turbulent model results in too much axial momentum diffusion relative to the experimental data. The turbulent results are fair considering the simple model used.

The above comparison shows that the simple turbulent model does an adequate job in accounting for transverse momentum diffusion. The discussion below will evaluate the effects of turbulent transverse momentum diffusion on certain types of subcompartment analysis using a hypothetical problem.

2. Hypothetical Problem. Consider the hypothetical containment subcompartment analysis problem shown in Fig. 15. In this problem, two subcompartments (volumes 1 and 2) are connected by a circular orifice as shown. In addition, volume 2 is connected to a bulk containment region by an identical orifice located on the geometric centerline of the orifice connecting volumes 1 and 2.

A high-energy blowdown in volume 1 would cause a rapid pressure build-up to occur that in turn would generate a high-energy jet flow into volume 2 through the orifice connecting the two volumes. The resultant differential pressure build-up between volume 2 and the bulk containment then would depend on the mass flow rate through the orifice connection between volume 2 and the bulk containment. If the computer code being used for this analysis does not account for the transverse momentum diffusion of the jet as it propagates across the volume, a higher mass flow rate would be calculated than if the code did account for transverse momentum diffusion. This in turn would result in differences in the calculated differential pressures between volume 2 and the bulk containment. A higher mass flow rate from volume 2 to the bulk containment results in a lower differential pressure build-up rather than a lower mass flow rate because the energy in the jet is convected out of volume 2 at a higher rate (assuming a constant flow rate into volume 2).

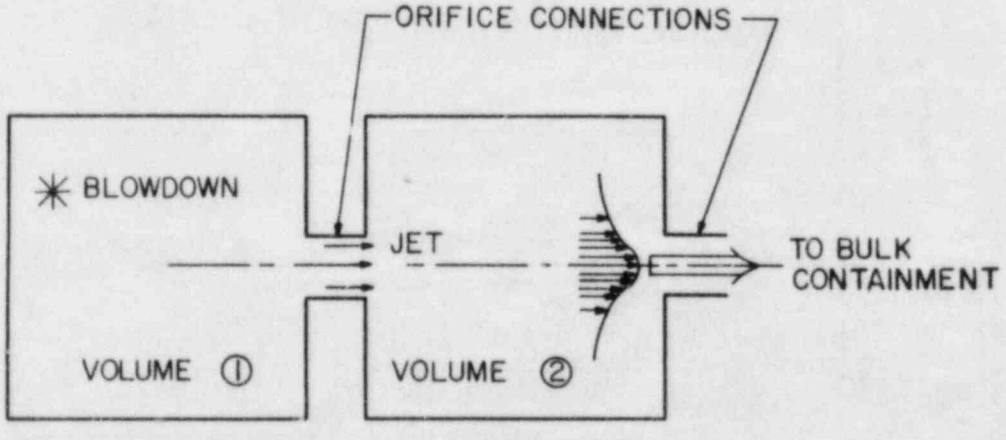

Fig. 15.
Schematic diagram of a hypothetical subcompartment analysis problem.

To substantiate this point, the hypothetical problem in Fig. 15 was modeled with the BEACON code for a constant jet of air entering volume 2 with a uniform velocity of 46.13 m/s and a radius of 0.5 m. The calculations were performed with and without the turbulent jet momentum diffusion model previously discussed. In addition, the problem also was modeled with the COMPARE code to assess the margin of conservatism in its calculations for applications to this type of geometry. The COMPARE assumptions correspond to total diffusion of the jet. Details of the BEACON and COMPARE models along with their respective input decks are included in Appendix B.

The effect of turbulent jet momentum diffusion on the mass flow rate between volume 2 and the bulk containment of the hypothetical problem is shown in Fig. 16. The computations were performed for a transient time period of 0.0 to 0.5 s, and the results are as expected. BEACON laminar calculations result in little or no momentum diffusion as the jet propagates across the volume; consequently, almost all of the jet's momentum leaves volume 2 through the orifice connecting it to the bulk containment. The turbulent jet momentum diffusion model results in a greater degree of transverse momentum diffusion. As a result, some of the momentum exits through the orifice, and the rest impinges on the wall surrounding the orifice, diffuses within the volume, and in effect reduces the mass flow rate relative to the laminar case. Both BEACON calculations predict the peak mass flow rate to occur at about 0.2 s. The peak mass flow rate for the laminar diffusion case is 23% greater than the peak mass flow rate for the turbulent diffusion case. The mass flow rate calculated by COMPARE is considerably less than either of the BEACON calculations. Consequently, COMPARE calculations for the differential pressure build-up will be higher than BEACON calculations because the rate at which energy is convected out of volume 2 will be lower than BEACON-calculated rates.

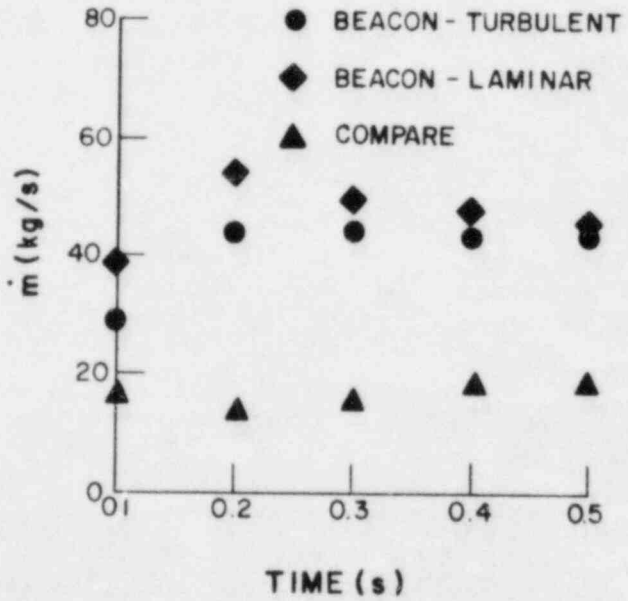

Fig. 16.
Effect of transverse turbulent momentum diffusion on BEACON-calculated mass flow rates for the hypothetical problem.

IV. CONCLUSIONS AND RECOMMENDATIONS

The analysis presented in this report revealed that significant differences do occur in reactor cavity forces and moments calculated by the COMPARE and BEACON codes. These differences are attributed directly to the differences in the calculated pressure fields that, in turn, are attributed to differences in modeling assumptions made by the two codes. Specifically, evaluation of the differences in calculated forces and moments for Geometry 1 showed that BEACON's capability to calculate a multidimensional flow-field along with the thermodynamics of a flashing liquid (chemical non-equilibrium) resulted in substantial differences in the distribution and magnitude of the pressure field relative to COMPARE calculations. The effects of mechanical and thermal non-equilibrium were negligible for this

geometry. As a result of the differences in the calculated pressure fields, the peak x-force calculated by COMPARE was greater (conservative) relative to BEACON's peak x-force calculation by 42%, whereas COMPARE's peak y-moment was opposite in sign and lower (less conservative) by 27% relative to BEACON. COMPARE calculations for peak forces and moments for Geometry 2 were both less than BEACON-calculated values by 64% and 36%, respectively. However, the BEACON calculations for Geometry 2, may have overestimated the forces and moments resulting from the modeling of the blowdown location. Based on the results of the calculations in this study, we conclude from comparison with the BEACON analyses that the COMPARE force and moment calculations for reactor cavity geometries involve margins that are indeterminate on a generic basis. That is, the difference between the calculations varies as a function of the specific geometry in question. In fact, because of the code models employed in some cases, COMPARE calculations may yield lower forces and moments than the best-estimate BEACON calculations.

We must emphasize that force-moment calculations for reactor cavity blowdown analysis are highly dependent on the geometry and nature of the thermodynamic processes that may occur as shown by differences in force-moment behavior of Geometries 1 and 2 discussed in this report. Therefore, if uncertainties exist as to the effect of geometry (for example, flow obstacles in the vicinity of the break) and nonequilibrium thermodynamics (for example, flashing liquid) on COMPARE calculations, we recommend that supporting calculations be done with a more advanced best-estimate code like BEACON in addition to performing sensitivity studies with COMPARE. (See Ref. 5.) Another option would be to perform COMPARE calculations that would maximize flow distribution; for example, use of critical flow options producing higher mass flows.

For general subcompartment analysis, accounting for turbulent jet momentum diffusion effects is necessary to accurately calculate mass flow rates with a multidimensional code like BEACON for geometries like the one considered in the hypothetical problem discussed in this report. However, COMPARE calculations for this type of geometry are conservative; that is, COMPARE-calculated mass flow rates are lower than BEACON-calculated mass flow rates.

REFERENCES

1. R. G. Gido, J. S. Gilbert, R. G. Lawton, and W. L. Jensen, "COMPARE-MOD1: A Code for the Transient Analysis of Volumes with Heat Sinks, Flowing Vents, and Doors," Los Alamos Scientific Laboratory report LA-7199-MS (March 1978).

2. R. G. Gido, G. J. E. Willcutt, Jr., J. L. Lunsford, and J. S. Gilbert, "COMPARE-MOD1 Code Addendum," Los Alamos National Laboratory report LA-7199-MS, NUREG/CR-1185 (August 1980), Addendum 1.

3. R. G. Gido and A. Koestal, "COMPARE Containment Subcompartment Analysis Code Evaluation," Proc. Int. Meeting on Thermal Nuclear Reactor Safety, Chicago, Illinois, August 29--September 2, 1982, US Nuclear Regulatory Commission report NUREG/CP-0027 (February 1983), Vol. 3, pp. 1583-1598

4. C. R. Broadus, R. J. Doyle, S. W. James, J. F. Lime, W. J. Mings, J. A. Ramsthaler, and M. S. Sahota, "BEACON/MOD3: A Computer Program for Thermal-Hydraulic Analysis of Nuclear Containments - User's Manual," EG G Idaho, Inc. report EGG-2008 (April 1980).

5. R. G. Gido, J. S. Gilbert, and C. G. Tinkler, "Subcompartment Analysis Procedures," Los Alamos Scientific Laboratory report LA-8169-MS, NUREG/CR-1199 (December 1979).

6. E. S. Idar, J. F. Lime, and R. G. Gido, "Comparison of COMPARE and BEACON Subcompartment Analyses of Battelle-Frankfurt Containment Tests," Los Alamos National Laboratory report LA-9461-MS, NUREG/CR-2849 (January 1983).

7. J. W. Bolstad, R. G. Gido, W. S. Gregory, P. E. Littleton, and G. J. E. Willcutt, Jr., "Comparison of COMPARE MOD1 Subcompartment Calculations with Battelle-Frankfurt D-Series Test Results," Los Alamos Scientific Laboratory report LA-8615-MS (December 1980).

8. R. G. Gido and A. Koestel, "Hydrogen Burn Analysis of Ice-Condenser Containments," Los Alamos National Laboratory report in preparation.

9. W. S. Gregory, J. R. Campbell, R. G. Gido, and A. J. Webb, "Comparison of COMPARE/RELAP3 Subcompartment Calculations with Battelle-Frankfurt C-Series Test Results," Los Alamos National Laboratory report LA-8866-MS, NUREG/CR-2177 (May 1981).

10. W. C. Rivard and M. D. Torrey, "Numerical Calculation of Flashing from Long Pipes Using a Two-Field Model," Los Alamos Scientific Laboratory report LA-6104-MS (November 1975).

11. J. O. Hinze and B. G. Van Der Hegge Zijnen, "Transfer of Heat and Matter in the Turbulent Mixing Zone of an Axially Symmetrical Jet," App. Scientific Res. (1949), Vol. A1, pp. 435-461.

APPENDIX A

BEACON MODELS AND INPUT SPECIFICATIONS USED FOR THE REACTOR CAVITY ANALYSIS

This appendix presents the BEACON models and input specifications used in the reactor cavity analysis of Sec. II. The BEACON model and input deck used for the reactor cavity Geometry 1 analysis can be found in Figs. A-1 and A-2, respectively. Figures A-3 and A-4 present the model and input deck for the shield-wall penetration of Geometry 2. The unwrapped reactor cavity annulus model for Geometry 2 and the corresponding BEACON input deck can be found in Figs. A-5 and A-6, respectively. Fig. A-7 presents the input specification used for the COMPARE SOURCE calculation for Geometry 2.

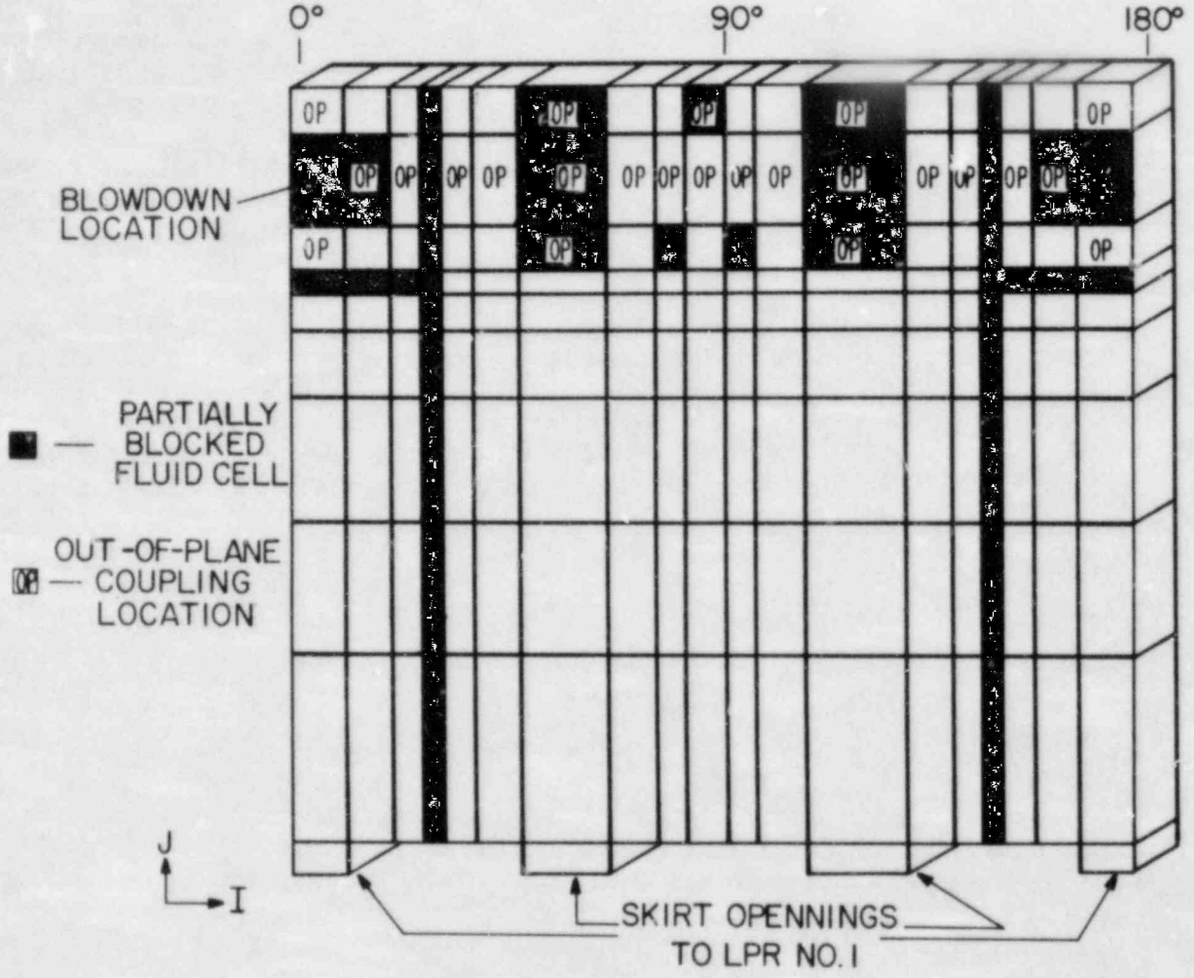

Fig. A-1.
BEACON reactor cavity model for Geometry 1.

```
100 'arkansas-1 reactor cavity analysis (hot leg break) '
*    timestep/execution/output interval parameters
105  noread,0,write,1,copy
110  0.0,0.10,0.0001,sec,20.0,1,noxeq,best
120  0.01,0.10
130  autodt,0,0.1,1.5,1.0e10
140  print,noprint,print,noprint,noprint,noprint
150  plots,1.0,1,1,0,0,0,0,0,0,1,0,0,0,0,0,0
190  29,1
200  1.0,0.00001,0.00001,100,5,5
240  lasl,pt,n/m2,degk,m,sec-1
* eulerian region input data
11000  cartsn,19,9,0.60,2.07,0.946,m,0.0,1.0
 21000  cartsn,1,1,0.669,0.525,0.60,m,0.0,1.0
 31000  cartsn,1,1,0.669,0.50,0.60,m,0.0,1.0
 41000  cartsn,1,1,0.669,1.0,0.50,m,0.0,1.0
 51000  cartsn,1,1,1.33,0.525,1.0,m,0.0,1.0
 61000  cartsn,1,1,1.33,1.0,0.50,m,0.0,1.0
 71000  cartsn,1,1,1.33,0.50,1.0,m,0.0,1.0
 81000  cartsn,1,1,1.33,1.0,0.50,m,0.0,1.0
 91000  cartsn,1,1,1.33,1.0,1.0,m,0.0,1.0
101000  cartsn,1,1,0.525,0.584,0.50,m,0.0,1.0
111000  cartsn,1,1,1.33,0.525,1.0,m,0.0,1.0
121000  cartsn,1,1,1.33,1.0,0.50,m,0.0,1.0
131000  cartsn,1,1,1.33,0.50,1.0,m,0.0,1.0
141000  cartsn,1,1,1.33,1.0,0.50,m,0.0,1.0
151000  cartsn,1,1,1.33,1.0,1.0,m,0.0,1.0
161000  cartsn,1,1,0.669,0.525,0.60,m,0.0,1.0
171000  cartsn,1,1,0.669,0.50,0.60,m,0.0,1.0
181000  cartsn,1,1,0.669,1.0,0.50,m,0.0,1.0
191000  cartsn,1,1,0.256,0.76,0.256,m,0.0,0.0
201000  cartsn,1,1,0.256,0.76,0.256,m,0.0,0.0
211000  cartsn,1,1,0.256,0.76,0.256,m,0.0,0.0
221000  cartsn,1,1,0.256,0.76,0.256,m,0.0,0.0
231000  cartsn,1,1,0.669,1.0,0.35,m,0.0,1.0
241000  cartsn,1,1,1.33,1.0,0.35,m,0.0,1.0
251000  cartsn,1,1,1.33,1.0,0.30,m,0.0,1.0
261000  cartsn,1,1,1.33,1.0,0.50,m,0.0,1.0
271000  cartsn,1,1,1.33,1.0,0.30,m,0.0,1.0
281000  cartsn,1,1,1.33,1.0,0.35,m,0.0,1.0
291000  cartsn,1,1,0.669,1.0,0.35,m,0.0,1.0
* variable mesh spacing
11020  0.60,0.50,0.35,0.20,0.35,0.50,1.0,0.50,0.30,
     + 0.50,0.30,0.50,1.0,0.50,0.35,0.20,0.35,0.50,0.60
11030  2.07,1.50,1.30,0.70,0.40,0.275,0.50,1.0,0.525
* fluid region input
11101  mixture,2,2,20,10,0,1.01353e5,311.0,311.0,1.000,0.96
 21101  mixture,2,2,2,2,0,1.01353e5,311.0,311.0,1.000,0.96
 31101  mixture,2,2,2,2,0,1.01353e5,311.0,311.0,1.000,0.96
 41101  mixture,2,2,2,2,0,1.01353e5,311.0,311.0,1.000,0.96
 51101  mixture,2,2,2,2,0,1.01353e5,311.0,311.0,1.000,0.96
 61101  mixture,2,2,2,2,0,1.01353e5,311.0,311.0,1.000,0.96
 71101  mixture,2,2,2,2,0,1.01353e5,311.0,311.0,1.000,0.96
 81101  mixture,2,2,2,2,0,1.01353e5,311.0,311.0,1.000,0.96
 91101  mixture,2,2,2,2,0,1.01353e5,311.0,311.0,1.000,0.96
101101  mixture,2,2,2,2,0,1.01353e5,311.0,311.0,1.000,0.96
111101  mixture,2,2,2,2,0,1.01353e5,311.0,311.0,1.000,0.96
121101  mixture,2,2,2,2,0,1.01353e5,311.0,311.0,1.000,0.96
131101  mixture,2,2,2,2,0,1.01353e5,311.0,311.0,1.000,0.96
141101  mixture,2,2,2,2,0,1.01353e5,311.0,311.0,1.000,0.96
151101  mixture,2,2,2,2,0,1.01353e5,311.0,311.0,1.000,0.96
161101  mixture,2,2,2,2,0,1.01353e5,311.0,311.0,1.000,0.96
171101  mixture,2,2,2,2,0,1.01353e5,311.0,311.0,1.000,0.96
181101  mixture,2,2,2,2,0,1.01353e5,311.0,311.0,1.000,0.96
```

Fig. A-2.
BEACON base-case input deck for the Geometry 1 reactor cavity model.

```
 65 191101  mixture,2,2,2,2,0,1.01353e5,311.0,311.0,1.000,0.96
 66 201101  mixture,2,2,2,2,0,1.01353e5,311.0,311.0,1.000,0.96
 67 211101  mixture,2,2,2,2,0,1.01353e5,311.0,311.0,1.000,0.96
 68 221101  mixture,2,2,2,2,0,1.01353e5,311.0,311.0,1.000,0.96
 69 231101  mixture,2,2,2,2,0,1.01353e5,311.0,311.0,1.000,0.96
 70 241101  mixture,2,2,2,2,0,1.01353e5,311.0,311.0,1.000,0.96
 71 251101  mixture,2,2,2,2,0,1.01353e5,311.0,311.0,1.000,0.96
 72 261101  mixture,2,2,2,2,0,1.01353e5,311.0,311.0,1.000,0.96
 73 271101  mixture,2,2,2,2,0,1.01353e5,311.0,311.0,1.000,0.96
 74 281101  mixture,2,2,2,2,0,1.01353e5,311.0,311.0,1.000,0.96
 75 291101  mixture,2,2,2,2,0,1.01353e5,311.0,311.0,1.000,0.96
 76 * restricted flow input
 77 * hot leg pipe-partial blockage
 78 11301  2,9,2,9,0.005,0.005,0.65
 79 11302  20,9,20,9,0.005,0.005,0.65
 80 *cold leg and core flood pipes-partial blockage
 81 11303  8,9,8,9,0.005,0.005,0.50
 82 11304  11,10,11,10,0.005,0.005,0.36
 83 11305  14,9,14,9,0.005,0.005,0.50
 84 * instrumentation (neutron detectors) piping-partial blockage
 85 11306  5,10,5,10,0.005,0.005,0.33
 86 11307  5,9,5,9,0.005,0.005,0.35
 87 11308  5,7,5,8,0.005,0.005,0.37
 88 11309  5,2,5,6,0.005,0.005,0.33
 89 11310  17,10,17,10,0.005,0.005,0.33
 90 11311  17,9,17,9,0.005,0.005,0.37
 91 11312  17,7,17,8,0.005,0.005,0.37
 92 11313  17,2,17,6,0.005,0.005,0.33
 93 * flow area and cell volume adjustments
 94 11314  3,9,3,9,0.005,0.005,0.50
 95 11315  2,7,2,7,0.005,0.005,0.10
 96 11316  3,7,3,7,0.005,0.005,0.10
 97 11317  4,7,4,7,0.005,0.005 0.10
 98 11318  8,10,8,10,0.005,0.005,0.45
 99 11319  8,8,8,8,0.005,0.005,0.20
100 11320  8,7,8,7,0.005,0.005,0.30
101 11321  10,8,10,8,0.005,0.005,0.50
102 11322  12,8,12,8,0.005,0.005,0.50
103 11323  14,10,14,10,0.005,0.005,0.45
104 11324  14,8,14,8,0.005,0.005,0.20
105 11325  14,7,14,7,0.005,0.005,0.30
106 11326  18,7,18,7,0.005,0.005,0.10
107 11327  19,7,19,7,0.005,0.005,0.10
108 11328  20,7,20,7,0.005,0.005,0.10
109 11329  19,9,19,9,0.0005,0.005,0.50
110 *  lumped parameter region input data
111 12000  zerod,64651.3,m3
112 12005  ' bulk containment '
113 12010  mixture,1.01353e5,311.0,311.0,1.000,0.96
114 * source cell input data
115 3010  liquid,1,2,9,3011,0.0 radians,0.5
116 3011  sec,lb/sec,btu/lb,ft,sec-1
117 3012  0.00000,1.14720e5,6.16160e2,0.0
118 3013  0.05005,1.05837e5,6.16405e2,0.0
119 3014  0.1000,1.0624e5,6.1785e2,0.0
120 3015  0.1500,1.0596e5,6.1910e2,0.0
121 3016  0.2001,1.0564e5,6.1908e2,0.0
122 3017  0.2500,1.0388e5,6.18791e2,0.0
123 3018  0.3000,1.0016e5,6.19009e2,0.0
124 3019  0.3500,1.0096e5,6.20047e2,0.0
125 3020  0.4001,1.0784e5,6.1944e2,0.0
126 3021  0.4500,1.0056e5,6.18138e2,0.0
127 3022  0.500,9.784e4,6.17743e2,0.0
128 3023  0.5501,9.760e4,6.17213e2,0.0
```

Fig. A-2.
BEACON base-case input deck for the Geometry 1 reactor cavity model (cont).

```
129 3024  0.600,9.760e4,6.14754e2,0.0
130 3025  0.6500,0.0,6.1207e2,0.0
131 3026  100.0,0.0,6.1207e2,0.0
132 3060  liquid,1,2,9,3061,0.0,radians,0.5
133 3061  sec,lb/sec,btu/lb,ft,sec-1
134 3062  0.0,0.0,6.1207e2,0.0
135 3063  0.6000,0.0,6.14754e2,0.0
136 3064  0.6500,9.744e4,6.1207e2,0.0
137 3065  0.7000,9.660e4,6.10766e2,0.0
138 3066  0.7501,9.420e4,6.10616e2,0.0
139 3067  0.8000,9.200e4,6.11304e2,0.0
140 3068  0.8500,9.1960e4,6.10265e2,0.0
141 3069  0.9001,9.032e4,6.1027e2,0.0
142 3070  0.9500,8.816e4,6.10708e2,0.0
143 3071  1.000,8.556e4,6.11033e2,0.0
144 3072  1.100,8.344e4,6.11697e2,0.0
145 3073  1.200,8.080e4,6.1287e2,0.0
146 3074  1.300,7.960e4,6.13568e2,0.0
147 3075  1.400,0.0,6.15584e2,0.0
148 3076  100.0,0.0,6.15584e2,0.0
149 *  region coupling input data
150 * eulerian region coupling
151 6001  bottom,1,2,2,1,19,2,2,1
152 6002  bottom,1,8,2,1,20,2,2,1
153 6003  bottom,1,14,2,1,21,2,2,1
154 6004  bottom,1,20,2,1,22,2,2,1
155 * lumped parameter region coupling
156 7001  left,2,2,2,1
157 7002  left,3,2,2,1
158 7003  left,4,2,2,1
159 7004  left,5,2,2,1
160 7005  left,6,2,2,1
161 7006  left,7,2,2,1
162 7007  left,8,2,2,1
163 7008  left,9,2,2,1
164 7009  left,10,2,2,1
165 7010  left,11,2,2,1
166 7011  left,12,2,2,1
167 7012  left,13,2,2,1
168 7013  left,14,2,2,1
169 7014  left,15,2,2,1
170 7015  left,16,2,2,1
171 7016  left,17,2,2,1
172 7017  left,18,2,2,1
173 7018  bottom,19,2,2,1
174 7019  bottom,20,2,2,1
175 7020  bottom,21,2,2,1
176 7021  bottom,22,2,2,1
177 7022  left,23,2,2,1
178 7023  left,24,2,2,1
179 7024  left,25,2,2,1
180 7025  left,26,2,2,1
181 7026  left,27,2,2,1
182 7027  left,28,2,2,1
183 7028  left,29,2,2,1
184 * out-of-plane coupling
185 8001  right,2,1,2,10
186 8002  right,3,1,2,8
187 8003  right,4,1,3,9
188 8004  right,5,1,8,10
189 8005  right,6,1,9,9
190 8006  right,7,1,8,8
191 8007  right,8,1,7,9
192 8008  right,9,1,8,9
```

Fig. A-2.
BEACON base-case input deck for the Geometry 1 reactor cavity model (cont).

```
193 8009  right,10,1,11,10
194 8010  right,11,1,14,10
195 8011  right,12,1,15,9
196 8012  right,13,1,14,8
197 8013  right,14,1,13,9
198 8014  right,15,1,14,9
199 8015  right,16,1,20,10
200 8016  right,17,1,20,8
201 8017  right,18,1,19,9
202 8018  right,23,1,4,9
203 8019  right,24,1,6,9
204 8020  right,25,1,10,9
205 8021  right,26,1,11,9
206 8022  right,27,1,12,9
207 8023  right,28,1,16,9
208 8024  right,29,1,18,9
209 * end of data input
210
```

Fig. A-2.
BEACON base-case input deck for the Geometry 1 reactor cavity model (cont).

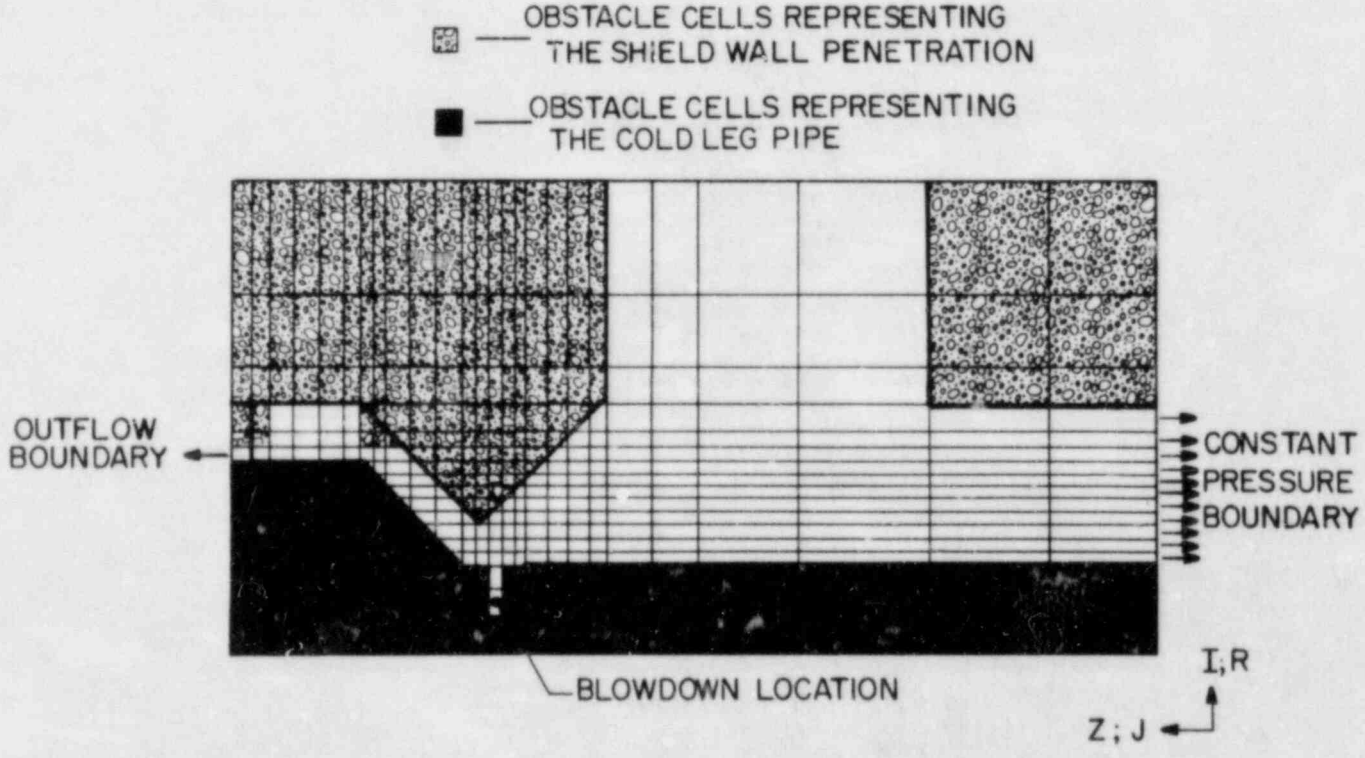

Fig. A-3.
BEACON shield-wall penetration model for Geometry 2.

```
100    'flour pioneer shield wall penetration flow model'
105    noread,0,write,1,copy
110    0.0,0.10,0.0001,sec,20.0,1,xeq,best
120    0.0025,0.02,0.005,0.10
130    autodt,0,0.1,1.5,1.0e10
140    print,noprint,print,noprint,noprint,noprint
150    plots,1.0,0,1,0.0,0,0,0,0,0,0,0,0,0,0,0
190    1,0
200    1.0,0.00001,0.00001,100,5,5
240    lasl,pt,lbf/in2,degr,ft,sec-1
*    eulerian region input data
11000    axisym,17,26,0.30,0.60,0.60,ft,0.0,0.0
11020    0.33,0.20,0.20,
      +0.10,0.10,0.10,0.10,0.10,0.10,0.10,0.10,0.10,0.12,0.25,
      +0.30,0.60,0.90
11030    0.90,0.90,1.10,0.80,0.40,0.35,0.17,0.17,0.17,0.17,
      +0.10,0.10,0.12,0.10,0.10,0.20,0.20,0.20,0.10,
      +0.10,0.15,0.20,0.20,0.20,0.15,0.15
*    fluid region input
11101    air,2,2,18,27,0,14.69,540.0
*    obstacle cells
11401    slip,2,2,4,13
11402    slip,16,2,18,3
11403    slip,2,14,2,27
11404    slip,3,15,4,27
11405    slip,5,17,5,27
11406    slip,6,18,7,27
11407    slip,8,19,9,27
11408    slip,10,20,11,27
11409    slip,12,21,12,27
11410    slip,8,15,8,15
11411    slip,9,14,9,16
11412    slip,10,13,10,16
11413    slip,11,12,11,17
11414    slip,12,11,12,17
11415    slip,13,11,13,18
11416    slip,14,10,14,21
11417    slip,15,9,15,21
11418    slip,16,8,18,27
11419    slip,14,26,15,27
*    boundary flow options
11501    constp,5,1,15,1
11502    outflow,13,28,13,28
11601    air,14.69,540.0
*    source cell input data
3010    liquid,1,3,14,3011,0.0,radians,1.0,1.0,1.0,0.0
3011    sec,lb/sec,btu/lb,ft,sec-1
3012    0.0,0.0,561.327,0.0
3013    2.5e-3,1.3586e4,561.327,0.0
3014    5.0e-3,1.794e4,561.376,0.0
3015    7.52e-3,2.1648e4,535.434,0.0
3016    1.001e-2,2.2913e4,561.131,0.0
3017    1.251e-2,2.4062e4,560.787,0.0
3018    1.501e-2,2.3856e4,559.717,0.0
3019    1.751e-2,2.6598e4,560.610,0.0
3020    2.003e-2,2.7096e4,560.015,0.0
3021    2.507e-2,2.6171e4,559.084,0.0
3022    3.005e-2,2.6676e4,558.742,0.0
3023    4.015e-2,2.8575e4,558.839,0.0
3024    4.508e-2,2.9015e4,558.749,0.0
3025    5.00e-2,0.0,558.749,0.0
3026    1000.0,0.0,558.749,0.0
3060    liquid,1,3,14,3061,0.0,radians,1.0,1.0,1.0,0.0
3061    sec,lb/sec,btu/lb,ft,sec-1
```

Fig. A-4.
BEACON input deck for the Geometry 2 shield-wall penetration model.

```
3062    0.0,0.0,558.749,0.0
3063    4.508e-2,0.0,558.749,0.0
3064    5.00e-2,2.8677e4,558.398,0.0
3065    6.003e-2,2.8188e4,557.975,0.0
3066    7.005e-2,2.6934e4,557.386,0.0
3067    8.005e-2,2.7439e4,557.620,0.0
3068    1.0013e-1,2.4419e4.556.455,0.0
3069    1.101e-1,2.4625e4,556.641,0.0
3070    1.201e-1,2.5466e4,557.012,0.0
3071    1.4005e-1,2.4539e4,556.569,0.0
3072    1.609e-1,2.3778e4,556.360,0.0
3073    1.8014e-1,2.3465e4,556.323,0.0
3074    2.001e-1,2.4322e4,556.685,0.0
3075    2.5003e-1,0.0,556.655,0.0
3076    1000.0,0.0,556.655,0.0
3110    liquid,1,3,14,3111,0.0,radians,1.0,1.0,1.0,0.0
3111    sec,lb/sec,btu/lb,ft,sec-1
3112    0.0,0.0,556.655,0.0
3113    2.001e-1,0.0,556.655,0.0
3114    2.5003e-1,2.4321e4,556.655,0.0
3115    3.0005e-1,2.4097e4,556.600,0.0
3116    4.0006e-1,2.3979e4,556.485,0.0
3117    5.0009e-1,2.428e4,556.583,0.0
```

Fig. A-4.
BEACON input deck for the Geometry 2 shield-wall penetration model (cont).

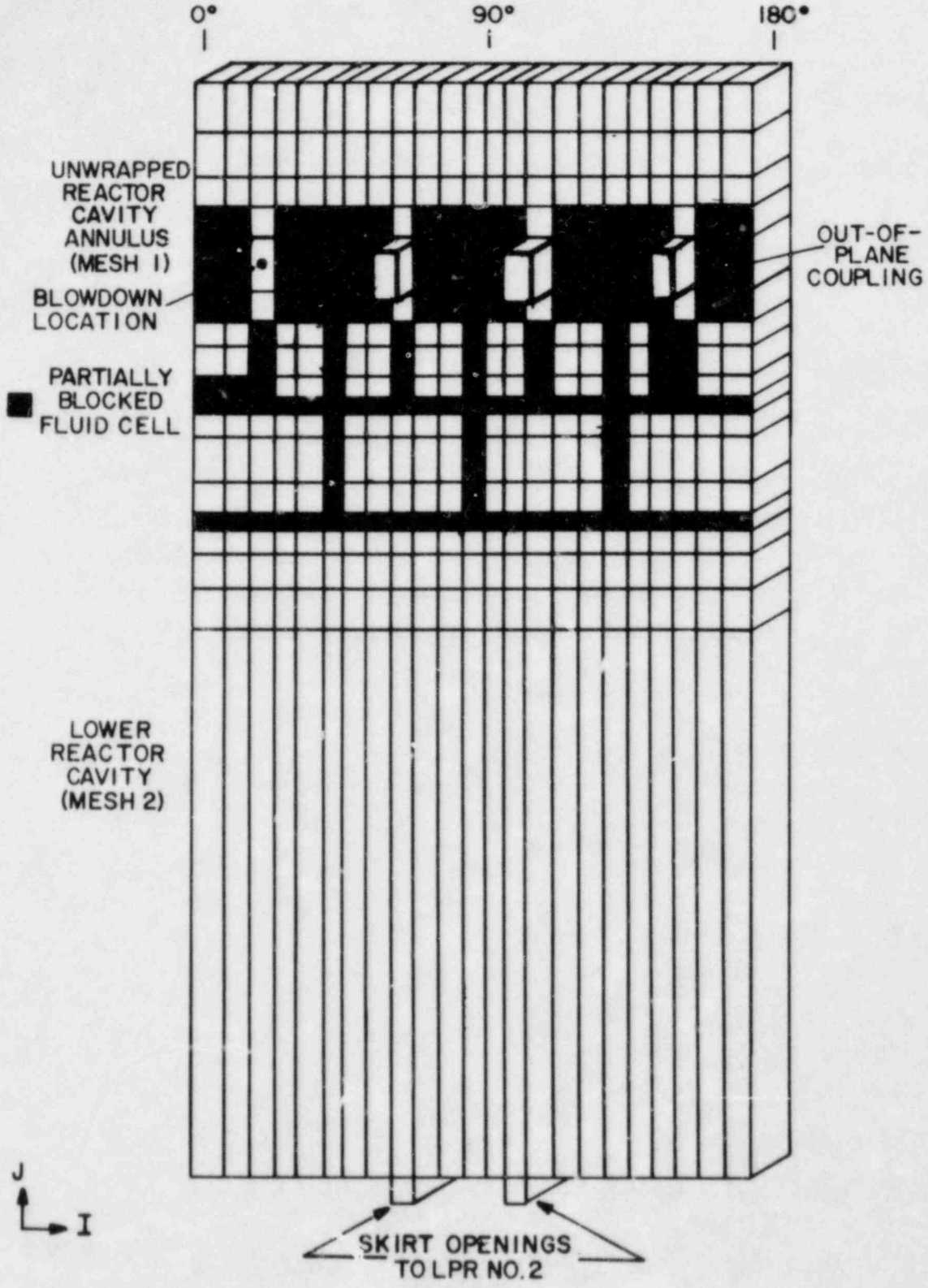

Fig. A-5.
BEACON reactor cavity model for Geometry 2.

```
100   'flour pioneer reactor cavity analysis (cold leg break)'
*   no form loss inputs
*   timestep/execution/output interval parameters
105   noread,0,write,1,copy
110   0.0,0.095,0.0001,sec,20.0,1,xeq,best
120   0.005,0.01,0.01,0.09,0.005,0.095
130   autodt,0,0.1,1.5,1.0e-4
140   print,noprint,print,noprint,noprint,noprint
150   plots,1.0,0,1,0,0,0,0,0,0,0,0,0,0,0,0
190   7,2
200   1.0,0.00001,0.00001,100,5,5
240   lasl,pt,lbf/in2,degr,ft,sec-1
* eulerian region input data
11000   cartsn,23,17,1.5708,1.80,0.60,ft,0.0,1.0
21000   cartsn,23,1,1.5708,24.00,0.60,ft,0.0,1.0
31000   cartsn,1,1,1.0,1.0,2.07,ft,0.0,1.0
41000   cartsn,1,1,1.0,1.0,1.39,ft,0.0,1.0
51000   cartsn,1,1,1.0,1.0,1.39,ft,0.0,1.0
61000   cartsn,1,1,1.0,1.0,0.60,ft,0.0,1.0
71000   cartsn,1,1,1.0,1.0,0.60,ft,0.0,1.0
*   variable mesh spacing (meshi)
11020   1.5708,1.0472,1.0472,1.0472,1.0472,1.0472,1.0472,
     +1.0472,1.0472,1.0472,1.0472,1.0472,1.0472,1.0472,
     +1.0472,1.0472,1.0472,1.0472,1.0472,1.0472,1.0472,
     +1.0472,1.5708
11030   1.80,1.50,1.00,0.70,1.40,2.00,1.00,0.70,1.00,1.320,
     +1.00,1.3835,2.400,1.3835,1.400,2.00,2.00
21020   1.5708,1.0472,1.0472,1.0472,1.0472,1.0472,1.0472
     +1.0472,1.0472,1.0472,1.0472,1.0472,1.0472,1.0472
     +1.0472,1.0472,1.0472,1.0472,1.0472,1.0472,1.0472
     +1.0472,1.5708
*   fluid region input
11101   mixture,2,2,24,18,0,14.69,534.7,534.7,1.000,0.96
21101   mixture,2,2,24,2,0,14.69,534.7,534.7,1.000,0.96
31101   mixture,2,2,2,2,0,14.69,534.7,534.7,1.000,0.96
41101   mixture,2,2,2,2,0,14.69,534.7,534.7,1.000,0.96
51101   mixture,2,2,2,2,0,14.69,534.7,534.7,1.000,0.96
61101   mixture,2,2,2,2,0,14.69,534.7,534.7,1.000,0.96
71101   mixture,2,2,2,2,0,14.69,534.7,534.7,1.000,0.96
*   restricted flow input (mesh 1)
*   pipe partial blockage
11301   2,13,2,13,0.02,0.02,0.90
11302   2,14,2,14,0.02,0.02,0.599
11303   2,15,2,15,0.02,0.02,0.90
11304   3,13,3,13,0.02,0.02,0.75
11305   3,14,3,14,0.02,0.02,0.89
11306   3,15,3,15,0.02,0.02,0.75
11307   5,13,5,13,0.02,0.02,0.75
11308   5,14,5,14,0.02,0.02,0.89
11309   5,15,5,15,0.02,0.02,0.75
11310   9,13,9,13,0.02,0.02,0.75
11311   9,14,9,14,0.02,0.02,0.89
11312   9,15,9,15,0.02,0.02,0.75
11313   11,13,11,13,0.02,0.02,0.75
11314   11,14,11,14,0.02,0.02,0.89
11315   11,15,11,15,0.02,0.02,0.75
11316   15,13,15,13,0.02,0.02,0.75
11317   15,14,15,14,0.02,0.02,0.89
11318   15,15,15,15,0.02,0.02,0.75
11319   17,13,17,13,0.02,0.02,0.75
11320   17,14,17,14,0.02,0.02,0.89
11321   17,15,17,15,0.02,0.02,0.75
11322   21,13,21,13,0.02,0.02,0.75
11323   21,14,21,14,0.02,0.02,0.89
```

Fig. A-6.
BEACON base-case input deck for the Geometry 2 reactor cavity model.

```
11324    21,15,21,15,0.02,0.02,0.75
11325    23,13,23,13,0.02,0.02,0.75
11326    23,14,23,14,0.02,0.02,0.89
11327    23,15,23,15,0.02,0.02,0.75
11328    24,13,24,13,0.02,0.02,0.90
11329    24,14,24,14,0.02,0.02,0.999
11330    24,15,24,15,0.02,0.02,0.90
*    flow area adjustments (mesh 1)
11331    4,16,4,18,0.02,0.02,0.01
11332    7,16,7,18,0.02,0.02,0.01
11333    10,16,10,18,0.02,0.02,0.01
11334    13,16,13,18,0.02,0.02,0.01
11335    16,16,16,18,0.02,0.02,0.01
11336    19,16,19,18,0.02,0.02,0.01
11337    22,16,22,18,0.02,0.02,0.01
11338    7,2,7,8,0.02,0.02,0.05
11339    13,2,13,8,0.02,0.02,0.05
11340    19,2,19,8,0.02,0.02,0.05
11341    2,5,24,5,0.02,0.02,0.18
11342    2,9,24,9,0.02,0.02,0.29
11343    4,10,4,12,0.02,0.02,0.14
11344    7,10,7,12,0.02,0.02,0.14
11345    10,10,10,12,0.02,0.02,0.14
11346    13,10,13,12,0.02,0.02,0.14
11347    16,10,16,12,0.02,0.02,0.14
11348    19,10,19,12,0.02,0.02,0.14
11349    22,10,22,12,0.02,0.02,0.14
11350    6,13,8,15,0.02,0.02,0.999
11351    12,13,14,15,0.02,0.02,0.999
11352    18,13,20,15,0.02,0.02,0.999
*    boundary flow options
11501     constp,2,19,20,19
11601     mixture,14.69,534.7,534.7,1.000,0.96
*    lumped parameter region input data
12000    zerod,1.694e6,ft3
12005    'upper containment'
12010    mixture,14.69,534.7,534.7,1.000,0.96
22000    zerod,15090.0,ft3
22005    ' lower containment '
22010    mixture,14.69,534.7,534.7,1.000,0.96
*    source cell input data
3010    liquid,1,4,14,3011,0.0,radians,0.5,1.0,1.0,0.0
3011    sec,kg/sec,j/kg,m,sec-1
3012     0.0,0.0,2.112e5,0.0
3013     2.5e-3,4.54e-4,2.112e5,0.0
3014     5.0e-3,73.61,8.724e5,0.0
3015     7.5e-3,312.79,8.458e5,0.0
3016     1.0e-2,528.90,8.994e5,0.0
3017     1.25e-2,720.34,9.417e5,0.0
3018     1.50e-2,871.68,9.753e5,0.0
3019     1.75e-2,991.12,1.003e6,0.0
3020     2.0e-2,1089.32,1.025e6,0.0
3021     2.5e-2,1236.95,1.059e6,0.0
3022     3.0e-2,1324.64,1.082e6,0.0
3023     3.5e-2,1379.05,1.098e6,0.0
3024     4.0e-2,1411.12,1.110e6,0.0
3025     4.5e-2,0.0,1.1195e6,0.0
3026     1000.0,0.0,1.1195e6,0.0
3060    liquid,1,4,14,3061,0.0,radians,0.5,1.0,1.0,0.0
3061    sec,kg/sec,j/kg,m,sec-1
3062     0.0,0.0,1.11e6,0.0
3063     4.0e-2,0.0,1.11e6,0.0
3064     4.5e-2,1430.55,1.1195e6,0.0
3065     5.0e-2,1442.16,1.127e6,0.0
```

Fig. A-6.
BEACON base-case input deck for the Geometry 2 reactor cavity model (cont).

```
3066     6.0e-2,1453.6,1.139e6,0.0
3067     7.0e-2,1451.15,1.236e6,0.0
3068     8.0e-2,1439.21,1.153e6,0.0
3069     9.0e-2,1424.31,1.157e6,0.0
3070     9.5e-2,1409.56,1.159e6,0.0
3110    steam,1,4,14,3111,0.0,radians,0.5,1.0,1.0,0.0
3111    sec,kg/sec,j/kg,m,sec-1
3112     0.0,0.0,3.25e5,0.0
3113     2.5e-3,7.046,3.25e5,0.0
3114     5.0e-3,51.04,1.706e6 0.0
3115     7.5e-3,105.93,2.7157e6,0.0
3116     1.0e-2,145.96,2.8075e6,0.0
3117     1.25e-2,172.43,2.8396e6,0.0
3118     1.5e-2,185.08,2.863e6,0.0
3119     1.75e-2,189.47,2.882e6,0.0
3120     2.0e-2,189.74,2.897e6,0.0
3121     2.5e-2,184.33,2.922e6,0.0
3122     3.0e-2,174.78,2.927e6,0.0
3123     3.5e-2,165.31,2.951e6,0.0
3124     4.0e-2,156.75,2.963e6,0.0
3125     4.5e-2,0.0,2.971e6,0.0
2126     1000.0,0.0,2.971e6,0.0
3160    steam,1,4,14,3161,0.0,radians,0.5,1.0,1.0,0.0
3161    sec,kg/sec,j/kg,m,sec-1
3162     0.0,0.0,2.963e6,0.0
3163     4.0e-2,0.0,2.963e6,0.0
3164     4.5e-2,149.43,2.971e6,0.0
3165     5.0e-2,142.71,2.979e6,0.0
3166     6.0e-2,131.41,2.991e6,0.0
3167     7.0e-2,122.73,3.023e6,0.0
3168     8.0e-2,116.05,3.010e6,0.0
3169     9.0e-2,110.87,3.014e6,0.0
3170     9.5e-2,108.40,3.017e6,0.0
*    region coupling input data
*    eulerian region coupling
6001    bottom,1,2,2,23,2,2,2,23
6002    bottom,2,10,2,1,6,2,2,1
6003    bottom,2,15,2,1,7,2,2,1
*    lumped parameter region coupling
7001    bottom,3,2,2,1
7002    bottom,4,2,2,1
7003    bottom,5,2,2,1
7004    bottom,6,2,2,2
7005    bottom,7,2,2,2
*    out-of-plane coupling
8001    top,3,1,10,14
8002    top,4,1,16,14
8003    top,5,1,22,14
```

Fig. A-6.
BEACON base-case input deck for the Geometry 2 reactor cavity model (cont).

```
100    'flour pioneer reactor cavity analysis (cold leg break)'
*    compare mass flows & enthalpy (mm=0.6)
*    timestep/execution/output interval parameters
105    noread,0,write,1,copy
110    0.0,0.10,0.0001,sec,20.0,1,xeq,best
120    0.005,0.01,0.01,0.10
130    autodt,0,0.1,1.5,1.0e-4
140    print,noprint,print,noprint,noprint,noprint
150    plots,1.0,0,1,0,0,0,0,0,0,0,0,0,0,0,0,0
190    7,2
200    1.0,0.00001,0.00001,100,5,5
240    lasl,pt,lbf/in2,degr,ft,sec-1
* eulerian region input data
11000    cartsn,23,17,1.5708,1.80,0.60,ft,0.0,1.0
21000    cartsn,23,1,1.5708,24.00,0.60,ft,0.0,1.0
31000    cartsn,1,1,1.0,1.0,2.07,ft,0.0,1.0
41000    cartsn,1,1,1.0,1.0,1.39,ft,0.0,1.0
51000    cartsn,1,1,1.0,1.0,1.39,ft,0.0,1.0
61000    cartsn,1,1,1.0,1.0,0.60,ft,0.0,1.0
71000    cartsn,1,1,1.0,1.0,0.60,ft,0.0,1.0
*    variable mesh spacing (mesh1)
11020    1.5708,1.0472,1.0472,1.0472,1.0472,1.0472,1.0472,
     +1.0472,1.0472,1.0472,1.0472,1.0472,1.0472,1.0472,
     +1.0472,1.0472,1.0472,1.0472,1.0472,1.0472,1.0472,
     +1.0472,1.5708
11030    1.80,1.50,1.00,0.70,1.40,2.00,1.00,0.70,1.00,1.320,
     +1.00,1.3835,2.400,1.3835,1.400,2.00,2.00
21020    1.5708,1.0472,1.0472,1.0472,1.0472,1.0472,1.0472
     +1.0472,1.0472,1.0472,1.0472,1.0472,1.0472,1.0472
     +1.0472,1.0472,1.0472,1.0472,1.0472,1.0472,1.0472
     +1.0472,1.5708
*    fluid region input
11101    mixture,2,2,24,18,0,14.69,534.7,534.7,1.000,0.96
21101    mixture,2,2,24,2,0,14.69,534.7,534.7,1.000,0.96
31101    mixture,2,2,2,2,0,14.69,534.7,534.7,1.000,0.96
41101    mixture,2,2,2,2,0,14.69,534.7,534.7,1.000,0.96
51101    mixture,2,2,2,2,0,14.69,534.7,534.7,1.000,0.96
61101    mixture,2,2,2,2,0,14.69,534.7,534.7,1.000,0.96
71101    mixture,2,2,2,2,0,14.69,534.7,534.7,1.000,0.96
*    restricted flow input (mesh 1)
*    pipe partial blockage
11301    2,13,2,13,0.02,0.02,0.90
11302    2,14,2,14,0.02,0.02,0.999
11303    2,15,2,15,0.02,0.02,0.90
11304    3,13,3,13,0.02,0.02,0.75
11305    3,14,3,14,0.02,0.02,0.89
11306    3,15,3,15,0.02,0.02,0.75
11307    5,13,5,13,0.02,0.02,0.75
11308    5,14,5,14,0.02,0.02,0.89
11309    5,15,5,15,0.02,0.02,0.75
11310    9,13,9,13,0.02,0.02,0.75
11311    9,14,9,14,0.02,0.02,0.89
11312    9,15,9,15,0.02,0.02,0.75
11313    11,13,11,13,0.02,0.02,0.75
11314    11,14,11,14,0.02,0.02,0.89
11315    11,15,11,15,0.02,0.02,0.75
11316    15,13,15,13,0.02,0.02,0.75
11317    15,14,15,14,0.02,0.02,0.89
11318    15,15,15,15,0.02,0.02,0.75
11319    17,13,17,13,0.02,0.02,0.75
11320    17,14,17,14,0.02,0.02,0.89
11321    17,15,17,15,0.02,0.02,0.75
11322    21,13,21,13,0.02,0.02,0.75
11323    21,14,21,14,0.02,0.02,0.89
```

Fig. A-7.
BEACON (COMPARE source) input deck for the Geometry 2 reactor cavity model.

```
11324    21,15,21,15,0.02,0.02,0.75
11325    23,13,23,13,0.02,0.02,0.75
11326    23,14,23,14,0.02,0.02,0.89
11327    23,15,23,15,0.02,0.02,0.75
11328    24,13,24,13,0.02,0.02,0.90
11329    24,14,24,14,0.02,0.02,0.999
11330    24,15,24,15,0.02,0.02,0.90
*    flow area adjustments (mesh 1)
11331    4,16,4,18,0.02,0.02,0.01
11332    7,16,7,18,0.02,0.02,0.01
11333    10,16,10,18,0.02,0.02,0.01
11334    13,16,13,18,0.02,0.02,0.01
11335    16,16,16,18,0.02,0.02,0.01
11336    19,16,19,18,0.02,0.02,0.01
11337    22,16,22,18,0.02,0.02,0.01
11338    7,2,7,8,0.02,0.02,0.05
11339    13,2,13,8,0.02,0.02,0.05
11340    19,2,19,8,0.02,0.02,0.05
11341    2,5,24,5,0.02,0.02,0.18
11342    2,9,24,9,0.02,0.02,0.29
11343    4,10,4,12,0.02,0.02,0.14
11344    7,10,7,12,0.02,0.02,0.14
11345    10,10,10,12,0.02,0.02,0.14
11346    13,10,13,12,0.02,0.02,0.14
11347    16,10,16,12,0.02,0.02,0.14
11348    19,10,19,12,0.02,0.02,0.14
11349    22,10,22,12,0.02,0.02,0.14
11350    6,13,8,15,0.02,0.02,0.999
11351    12,13,14,15,0.02,0.02,0.999
11352    18,13,20,15,0.02,0.02,0.999
*    boundary flow options
11501     constp,2,19,20,19
11601     mixture,14.69,534.7,534.7,1.000,0.96
*    lumped parameter region input data
12000    zerod,1.694e6,ft3
12005    'upper containment'
12010    mixture,14.69,534.7,534.7,1.000,0.96
22000    zerod,15090.0,ft3
22005    ' lower containment '
22010    mixture,14.69,534.7,534.7,1.000,0.96
*    source cell input data
3010    liquid,1,4,14,3011,0.0,radians,1.0,1.0,1.0,0.0
3011    sec,kg/sec,j/kg,m,sec-1
3012     0.0,0.0,0.0,0.0
3013     2.0e-3,1.127,1.6143e5,0.0
3014     4.0e-3,24.386,1.1722e5,0.0
3015     5.0e-3,40.41,1.0958e6,0.0
3016     1.0e-2,131.83,9.17545e5,0.0
3017     1.5e-2,214.42,8.7136e5,0.0
3018     2.0e-2,266.97,8.4824e5,0.0
3019     3.0e-2,337.96,8.195e5,0.0
3020     4.0e-2,393.07,8.0303e5,0.0
3021     5.0e-2,426.65,7.9376e5,0.0
3022     6.0e-2,434.58,7.8967e5,0.0
3023     7.0e-2,425.56,7.8855e5,0.0
3024     8.0e-2,414.10,7.8946e5,0.0
3025     9.0e-2,409.77,7.89536e5,0.0
3026     1.0e-1,387.82,8.3292e5,0.0
3060    steam,1,4,14,3061,0.0,radians,1.0,1.0,1.0,0.0
3061    sec,kg/sec,j/kg,m,sec-1
3062     0.0,0.0,0.0,0.0
3063     2.0e-3,0.999,1.8211e6,0.0
3064     4.0e-3,15.143,1.88767e5,0.0
3065     5.0e-3,22.51,1.9672e6,0.0
```

Fig. A-7.
BEACON (COMPARE source) input deck for the Geometry 2 reactor cavity model (cont).

```
3066     1.0e-2,49.744,2.43165e6,0.0
3067     1.5e-2,67.70,2.760e6,0.0
3068     2.0e-2,76.11,2.9754e6,0.0
3069     3.0e-2,84.19,3.2897e6,0.0
3070     4.0e-2,89.87,3.5123e6,0.0
3071     5.0e-2,92.68,3.654e6,0.0
3072     6.0e-2,92.88,3.6948e6,0.0
3073     7.0e-2,91.34,3.674e6,0.0
3074     8.0e-2,90.04,3.631e6,0.0
3075     9.0e-2,89.39,3.620e6,0.0
3076     1.0e-1,86.86,3.719e6,0.0
*   region coupling input data
*   eulerian region coupling
6001   bottom,1,2,2,23,2,2,2,23
6002   bottom,2,10,2,1,6,2,2,1
6003   bottom,2,15,2,1,7,2,2,1
*   lumped parameter region coupling
7001   bottom,3,2,2,1
7002   bottom,4,2,2,1
7003   bottom,5,2,2,1
7004   bottom,6,2,2,2
7005   bottom,7,2,2,2
*   out-of-plane coupling
8001   top,3,1,10,14
8002   top,4,1,16,14
8003   top,5,1,22,14
```

Fig. A-7.
BEACON (COMPARE source) input deck for the Geometry 2 reactor cavity model (cont).

APPENDIX B

BEACON AND COMPARE MODELS AND INPUT SPECIFICATIONS USED FOR THE TURBULENT JET DIFFUSION EFFECTS ANALYSIS

This appendix discusses the BEACON and COMPARE models and input specifications used for the analysis presented in Sec. III.B in this report.

The BEACON model for the circular free jet analysis of Sec. III.B.1 is shown in Fig. B-1. The model used an axisymmetric geometry with 504 interior cells to model the fluid region. An inflow boundary with five cells was used to model a uniform velocity circular jet entering the fluid region; boundary conditions are used as indicated in the figure. The jet radius and inflow velocity are 0.5 m and 46.3 m/s, respectively. The input decks associated with the model for both laminar and turbulent jet calculations are shown in Figs. B-2(a) and B-2(b).

The BEACON model for the hypothetical problem discussed in Sec. III.B.2 is shown in Fig. B-3. This model was obtained by taking the free jet model of Fig. B-1 and adding an obstacle region, which is shown by the shaded cells in Fig. B-3. The fluid region to the left of the obstacle region represents volume 2 of the hypothetical problem shown in Fig. 15, whereas the fluid region to the right of the obstacle region represents the bulk containment of the hypothetical problem. The small fluid region between the top of the obstacle region and the rigid/slip boundary models the orifice connnection between volume 2 and the bulk containment. The inflow boundary models the jet entering volume 2 as a result of a hypothetical blowdown in volume 1 in Fig. 15. The BEACON input decks for both laminar and turbulent jet calculations for the model in Fig. B-3 are shown in Figs. B-4(a) and B-4(b).

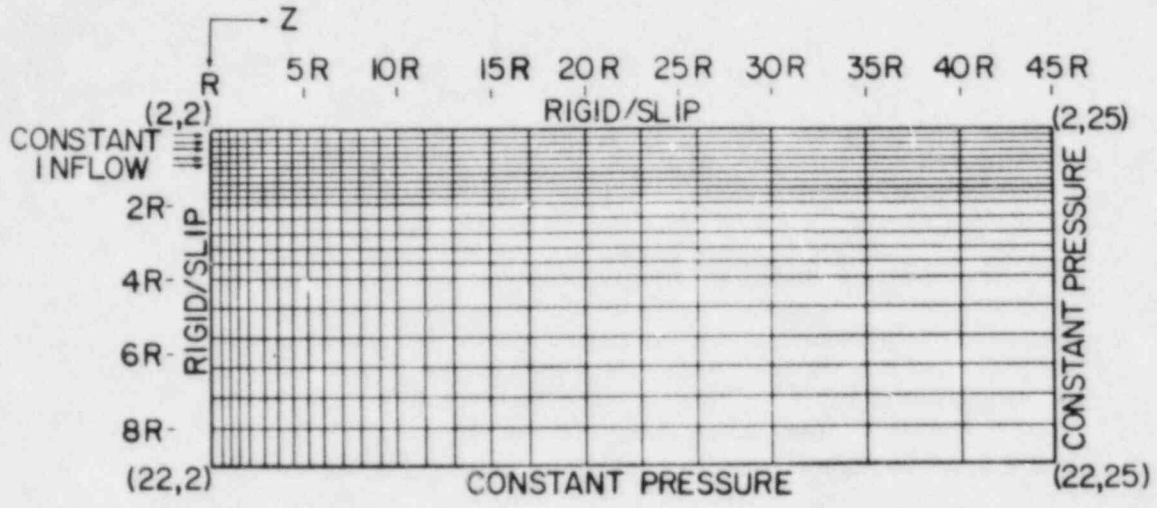

Fig. B-1.
BEACON model for a circular free jet of air (R = 0.5 m).

```
100  'axisymmetric jet analysis - laminar'
105  noread  0  write  1  copy
110  0.0  0.5  0.00001  sec  20.0  1  xeq  best
120  0.1  0.5
130  autodt  0  0.1  1.5  1.0e10
140  print  print  print  noprint  noprint  noprint
150  plots  1.0 0 0 0 0 0 0 0 0 0 0 0 0 0 0 0
190  1
200  1.0  0.00001  0.00001  50  5  5
240  lasl  pt  lbf/in2  degf  ft  sec-1
270  0.0  0.0  46.318  0.5
******mesh data******
11000  axisym  21  24  0.1  0.25  0.0  m  0.0  0.0
11010  slip  slip  slip  slip
11020  0.1 0.1 0.1 0.1 0.1 0.1 0.1 0.1 0.1 0.1 0.2 0.2 0.2 0.2 0.2 0.2
+      0.4 0.4 0.4 0.4 0.5
11030  0.25 0.25 0.25 0.25 0.4 0.4 0.4 0.4 0.4 0.5 0.5 0.5 0.5 0.75 0.75
+      1.0 1.0 1.5 1.5 1.5 2.0 2.5 2.5 2.5
11101  air 2 2  22 25  0 14.7  70.0
11501  inflow  2 1  6 1
11502  constp  23 1  23 26
11503  constp  1 26  22 26
11601  air  14.8  501.0
11602  air  14.7  70.0
11603  air  14.7  70.0
11701  0.0  151.962  0.0  151.962
******end of data input******
```

Fig. B-2(a).
BEACON input deck for a laminar circular free jet model.

```
100  'axisymmetric jet analysis - turbulent * 1.0'
105  noread  0  write  1  copy
110  0.0  0.5  0.00001  sec  20.0  1  xeq  best
120  0.1  0.5
130  autodt  0  0.1  1.5  1.0e10
140  print  print  print  noprint  noprint  noprint
150  plots  1.0 0 0 0 0 0 0 0 0 0 0 0 0 0 0 0 0 0
190  1
200  1.0  0.00001  0.00001  50  5  5
240  lasl  pt  lbf/in2  degf  ft  sec-1
270  1.0  1.0  46.318  0.5
******mesh data******
11000  axisym  21  24  0.1  0.25  0.0  m  0.0  0.0
11010  slip  slip  slip  slip
11020  0.1 0.1 0.1 0.1 0.1 0.1 0.1 0.1 0.1 0.1 0.2 0.2 0.2 0.2 0.2 0.2
+      0.4 0.4 0.4 0.4 0.5
11030  0.25 0.25 0.25 0.25 0.4 0.4 0.4 0.4 0.4 0.5 0.5 0.5 0.5 0.75 0.75
+      1.0 1.0 1.5 1.5 1.5 2.0 2.5 2.5 2.5
11101  air 2 2  22 25  0 14.7  70.0
11501  inflow  2 1  6 1
11502  constp  23 1  23 26
11503  constp  1 26  22 26
11601  air  14.8  501.0
11602  air  14.7  70.0
11603  air  14.7  70.0
11701  0.0  151.962  0.0  151.962
******end of data input******
```

Fig. B-2(b).
BEACON input deck for a turbulent circular free jet model.

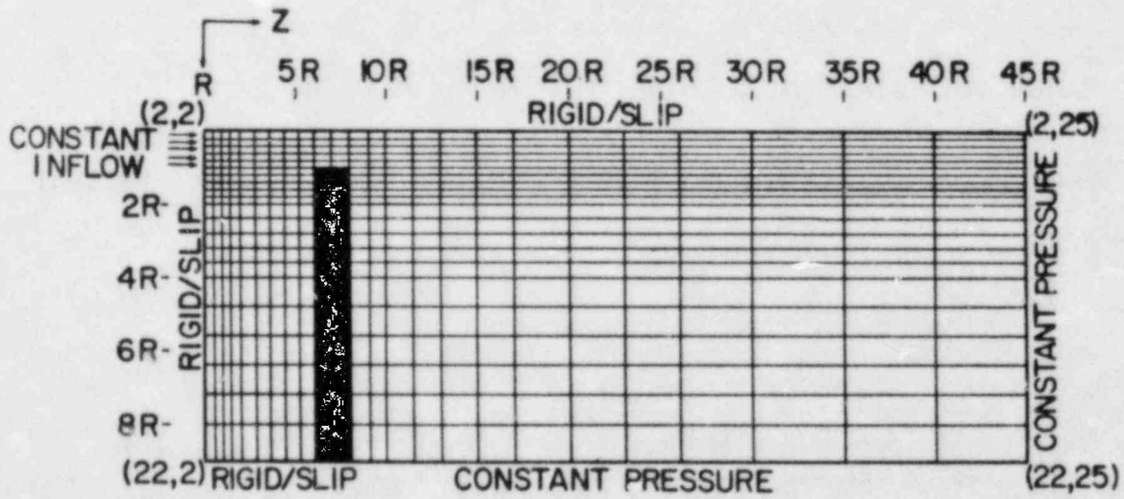

Fig. B-3.
BEACON model for the hypothetical jet problem (R = 0.5 m).

```
100  'axisymmetric jet analysis - laminar'
105  noread  0  write  1  copy
110  0.0  0.5  0.00001  sec  20.0  1  xeq  best
120  0.1  0.5
130  autodt  0  0.1  1.5  1.0e10
140  print  print  print  noprint  noprint  noprint
150  plots  1.0 0 0 0 0 0 0 0 0 0 0 0 0 0 0 0 0
190  1
200  1.0  0.00001  0.00001  50  5  5
240  lasl  pt  lbf/in2  degf  ft  sec-1
270  0.0  0.0  46.318  0.5
******mesh data******
11000  axisym  21  24  0.1  0.25  0.0  m  0.0  0.0
11010  slip  slip  slip  slip
11020  0.1 0.1 0.1 0.1 0.1 0.1 0.1 0.1 0.1 0.1 0.2 0.2 0 2 0.2 0.2 0.2
+      0.4 0.4 0.4 0.4 0.5
11030  0.25 0.25 0.25 0.25 0.4 0.4 0.4 0.4 0.4 0.5 0.5 0.5 0.5 0.75 0.75
+      1.0 1.0 1.5 1.5 1.5 2.0 2.5 2.5 2.5
11101  air 2 2  22 10  0 14.7  70.0
11102  air 2 11  6 12  0 14.7  70.0
11103  air 2 13  22 25  0 14.7 70.0
11401  slip 7 11  22 12
11501  inflow  2 1  6 1
11502  constp  23 13  23 26
11503  constp  1 26  22 26
11601  air  14.8  70.14
11602  air  14.7  70.0
11603  air  14.7  70.0
11701  0.0  151.962  0.0  151.962
******end of data input******
```

Fig. B-4(a).
BEACON input deck for the laminar jet calculation for the hypothetical problem.

```
100  'axisymmetric jet analysis - turbulent * 1.0'
105  noread  0  write  1  copy
110  0.0  0.5  0.00001  sec  20.0  1  xeq  best
120  0.1  0.5
130  autodt  0  0.1  1.5  1.0e10
140  print  print  print  noprint  noprint  noprint
150  plots  1.0 0 0 0 0 0 0 0 0 0 0 0 0 0 0 0 0
190  1
200  1.0  0.00001  0.00001  50  5  5
240  lasl  pt  lbf/in2  degf  ft  sec-1
270  1.0  1.0  46.318  0.5
******mesh data******
11000  axisym  21  24  0.1  0.25  0.0  m  0.0  0.0
11010  slip  slip  slip  slip
11020  0.1 0.1 0.1 0.1 0.1 0.1 0.1 0.1 0.1 0.1 0.2 0.2 0.2 0.2 0.2 0.2
+      0.4 0.4 0.4 0.4 0.5
11030  0.25 0.25 0.25 0.25 0.4 0.4 0.4 0.4 0.4 0.5 0.5 0.5 0.5 0.75 0.75
+      1.0 1.0 1.5 1.5 1.5 2.0 2.5 2.5 2.5
11101  air 2 2  22 10  0 14.7  70.0
11102  air 2 11  6 12  0 14.7  70.0
11103  air 2 13  22 25  0 14.7 70.0
11401  slip 7 11  22 12
11501  inflow  2 1  6 1
11502  constp  23 13  23 26
11503  constp  1 26  22 26
11601  air  14.8  70.14
11602  air  14.7  70.0
11603  air  14.7  70.0
11701  0.0  151.962  0.0  151.962
******end of data input******
```

Fig. B-4(b).
BEACON input deck for the turbulent jet calculation for the hypothetical problem.

The COMPARE model for the hypothetical problem of Fig. 15 is shown in Fig. B-5. In this model V_1 and V_2 correspond to volume 1 and volume 2 in Fig. 15. V_4 represents the bulk containment, and V_3 represents the orifice connection between volume 2 and the bulk containment. The jet entering volume 2 is modeled by COMPARE as a mass and energy source located in V_2. The input deck for the COMPARE model is shown in Fig. B-6.

All volumes, flow areas, and inital conditions are consistent between the BEACON and COMPARE models for the hypothetical problem in Fig. 15.

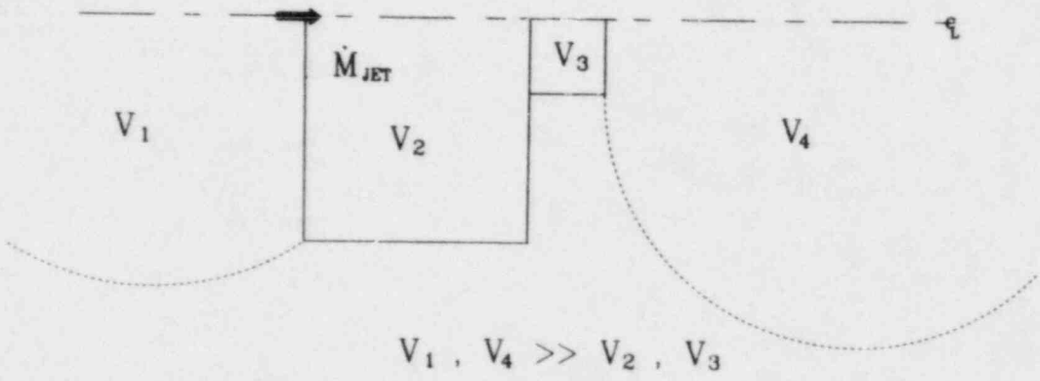

Fig. B-5.
COMPARE model for the hypothetical jet problem.

```
LISTING OF INPUT CARDS

LINENO  COL-5    10    15    20    25    30    35    40    45    50    55    60    65    70    75    80  LINENO
     1  JET - SOURCE IS BLOWDOWN OF N2 AND O2 AT 70F                                                        1
     2       4     1     0     0     2     0     0     0     0     0     1     T                           2
     3       100000      2     1   0.0       .8          .010        .001        0.                        3
     4  1.          .001                5000                                                              4
     5     1.E10      14.8   501.      0.                                                                 5
     6   6739.80      14.7    70.                                                                        6
     7     27.736     14.7    70.                                                                        7
     8     1.E10      14.7    70.                                                                        8
     9       1     1     2     0     0                                                                   9
    10  0.000       0.          1.          .5          1.          0.          0.                        10
    11      1     2     3     0     0                                                                   11
    12  8.454        .5          0.          .0          1.          0.          0.                        12
    13      1     3     4     0     0                                                                   13
    14  8.454        0.          1.          .5          0.          0.          0.                        14
    15      2     2     1     2     2     2                                                             15
    16  0.          41.920      070.        100.        41.920      070.                                  16
    17  0.          11.110      070.        100.        11.110      070.                                  17
    18      1     1     1     1     0     0     0  1000     1   100   200     0                          18
    19  0.           .8          8.                                                                     19
    20  1    6.     14.5    15.7      2     3     4                                                      20
    21  2    6.     60.     180.      2     3     4                                                      21
    22  3    6.   -150.     150.      2     3                                                            22
    23  4    6.    -0.6      0.6      2     3     3     4                                                23
    24                                                                                                  24
    25                                                                                                  25
    26                                                                                                  26
    27                                                                                                  27
    28                                                                                                  28
    29                                                                                                  29

LINENO  COL-5    10    15    20    25    30    35    40    45    50    55    60    65    70    75    80  LINENO
```

Fig. B-6.
COMPARE input deck for the hypothetical problem.

NRC FORM 335 (11-81)

U.S. NUCLEAR REGULATORY COMMISSION

BIBLIOGRAPHIC DATA SHEET

1. REPORT NUMBER *(Assigned by DDC)*
NUREG/CR-3305
LA-9776-MS

4. TITLE AND SUBTITLE *(Add Volume No., if appropriate)*
Comparison of BEACON and COMPARE Reactor Cavity Subcompartment Analyses

2. *(Leave blank)*

3. RECIPIENT'S ACCESSION NO.

7. AUTHOR(S)
M. W. Burkett, E.S. Idar, R. G. Gido, J. F. Lime, and A. Koestel

5. DATE REPORT COMPLETED
MONTH: February YEAR: 1984

9. PERFORMING ORGANIZATION NAME AND MAILING ADDRESS *(Include Zip Code)*
Los Alamos National Laboratory
Los Alamos, New Mexico 87545

DATE REPORT ISSUED
MONTH: April YEAR: 1984

6. *(Leave blank)*

8. *(Leave blank)*

12. SPONSORING ORGANIZATION NAME AND MAILING ADDRESS *(Include Zip Code)*
Division of Systems Integration
Office of Nuclear Reactor Regulation
U.S. Nuclear Regulatory Commission
Washington, D.C. 20555

10. PROJECT/TASK/WORK UNIT NO.

11. FIN NO.
A-7265

13. TYPE OF REPORT
Technical

PERIOD COVERED *(Inclusive dates)*

15. SUPPLEMENTARY NOTES

14. *(Leave blank)*

16. ABSTRACT *(200 words or less)*

In this study, a more advanced "best-estimate" containment code, BEACON-MOD3A, was used to calculate force and moment loads resulting from a high-energy blowdown for two reactor cavity geometries previously analyzed with the licensing computer code COMPARE-MOD1A. The BEACON force and moment loads were compared with the COMPARE results to determine the safety margins provided by the COMPARE code. The forces and moments calculated by the codes were found to be different, although not in any consistent manner, for the two reactor cavity geometries studied. Therefore, generic summary statements regarding margins cannot be made because of the effects of the detailed physical configuration. However, differences in the BEACON and COMPARE calculated forces and moments can be attributed to differences in the modeling assumptions used in the codes and the analyses.

17. KEY WORDS AND DOCUMENT ANALYSIS

17a. DESCRIPTORS

17b. IDENTIFIERS/OPEN-ENDED TERMS

18. AVAILABILITY STATEMENT
Unlimited

19. SECURITY CLASS *(This report)*
Unclassified

21. NO. OF PAGES

20. SECURITY CLASS *(This page)*
Unclassified

22. PRICE
$

NRC FORM 335 (11-81)

UNITED STATES
NUCLEAR REGULATORY COMMISSION
WASHINGTON, D.C. 20555

OFFICIAL BUSINESS
PENALTY FOR PRIVATE USE, $300

FOURTH-CLASS MAIL
POSTAGE & FEES PAID
USNRC
WASH. D.C.
PERMIT No. G-67

120555078877 1 1AN1R2
US NRC
ADM-DIV OF TIDC
POLICY & PUB MGT BR-PDR NUREG
W-501
WASHINGTON DC 20555